

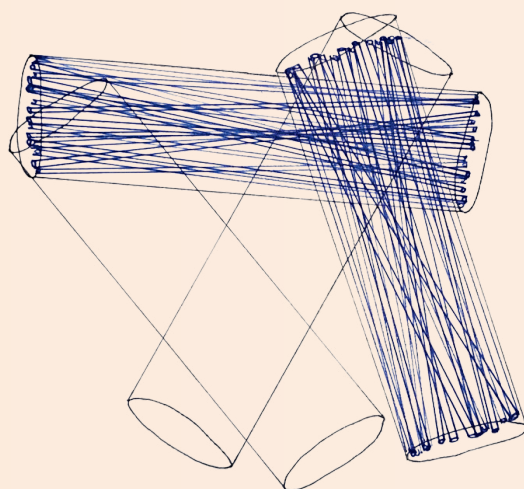
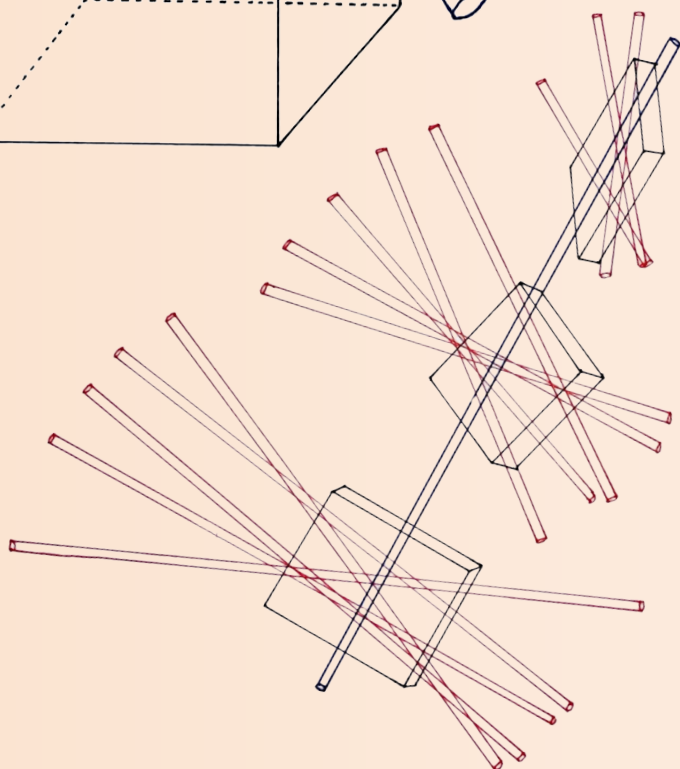
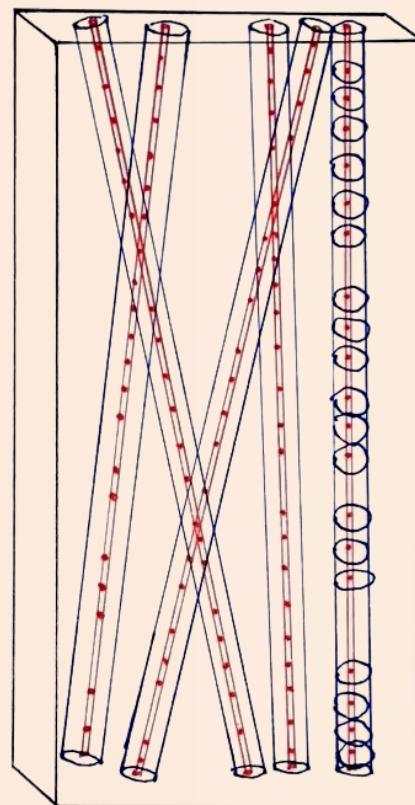
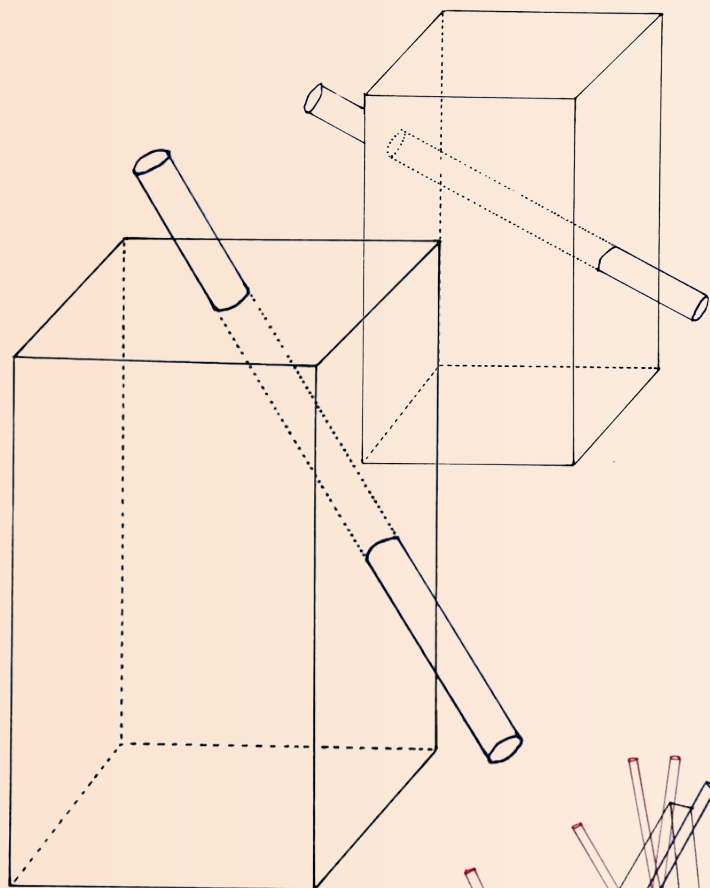
McGill Undergraduate Mathematics Journal



the δ elta ϵ psilon

Spring 2025

Eighth Issue



Copyright © *The Delta Epsilon*, 2025

All rights reserved. The text of this publication may not be reproduced in any form or by any means without prior written consent of the authors and of *The Delta Epsilon*.

Issue 8, published March 20th, 2025

ISSN: 1911-8996

LETTER FROM THE EDITORS

You thought you'd be waiting ∞ for the next issue of *The Delta Epsilon*, but you were looking at it sideways:

8 is right here!

We are thrilled to finally publish a new issue of *The Delta Epsilon* for the first time in over a decade. We felt as though there was a hole in the soul of the mathematical community here at McGill that was the unique shape of the Greek letters δ and ϵ . Though there were many perturbations in the road, our blood, sweat, and L^AT_EX compilation errors were worth it to be able to provide a place for undergraduates to showcase their excellence. On top of that, this journal contains pearls of wisdom from your favourite professors as well as many brain teasers and jokes scattered throughout to unwind between articles.

If you'd like to be featured in the next issue, we encourage you to submit articles next year or apply to be on our editorial board. It's been a blast compiling this issue for you guys.

We hope you enjoy all the hard work that has gone into the publishing of this issue. Make sure you read this cover-to-cover so you don't miss any of the hidden treasures.

Sincerely,
Helena and Hy, Editors-in-Chief
(On behalf of the editorial team)



LETTER FROM SUMS

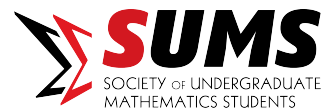
An undergraduate academic journal provides aspiring researchers with invaluable opportunities to learn how to conduct, write, and publish research while gaining recognition for their efforts. For these reasons, I am deeply grateful to the many individuals whose dedication has made the revival of *The Delta Epsilon* possible.

A decade has passed since its last publication, and reviving the journal has been no small undertaking. I extend my sincere gratitude to Nicholas Hayek, whose leadership and commitment were instrumental in bringing *The Delta Epsilon* back to life. Alongside Charlotte Weiss, he recruited and mentored editors, and ensured the journal's preservation. Their efforts have been an inspiration to us all.

Special thanks to Helena Heinonen and Hy Vu, this year's editors-in-chief, who faced the unique challenge of re-establishing the editorial process from the ground up. Their exceptional work has set a strong precedent for future editors and solidified the journal's foundation for years to come.

On behalf of the Society of Undergraduate Mathematics Students, I congratulate all contributing students on this remarkable achievement. The articles submitted to *The Delta Epsilon* stand as a testament to the initiative, determination, and intellectual curiosity of McGill's undergraduate mathematics community.

Sincerely,
Pilar DaRonco, SUMS President
(On behalf of the SUMS council)



THE δ ELTA ϵ PSILON

MCGILL UNDERGRADUATE MATHEMATICS JOURNAL

CONTENTS

Riesz-Thorin Interpolation & Applications	1
<i>Anson Li and Mohamed-Amine Azzouz</i>	
Modelling Baseball Exit Velocities with Block Maxima	8
<i>Jules Lanari-Collard</i>	
Interview with Jean Pierre Mutanguha	13
<i>Helena Heinonen and Aahaan Rawal</i>	
Inertial Gravity Wave Derivation and Model Implementation	16
<i>Jelena Collins</i>	
Fractal Geometry: The Exploration of Julia Sets	21
<i>Gabriella Chen</i>	
Rethinking Mathematical Progress with Lakatos	31
<i>Natan Sakajiri</i>	
Computational Aspects of Modular Forms	34
<i>Ben Merbaum</i>	
Interview with Sidney Trudeau	39
<i>Elizabeth van Oorschot</i>	
Fourier Analysis: The Catalyst of Modern Analysis	41
<i>Nisrine Sqalli and Samy Lahlou</i>	
Crossword	48
<i>Helena Heinonen</i>	
Solution to Puzzles	49
Acknowledgements	51

RIESZ-THORIN INTERPOLATION & APPLICATIONS

Anson Li and Mohamed-Amine Azzouz

This article establishes the Riesz-Thorin interpolation theorem, which states that the stability and boundedness of a L^p linear operator can be deduced “from the endpoints.” Two applications are also discussed: (i) Hausdorff-Young inequality for Fourier transforms and (ii) boundedness of conditional expectation operators across L^p spaces (without the use of Jensen’s inequality). The last section contains a summary of the proof techniques used, along with various functional analytic generalizations of the main results to semifinite or finitely-additive measure spaces.

INTRODUCTION

The Riesz-Thorin interpolation theorem is a theorem in functional analysis that enables one to deduce the properties of a linear operator T ‘in between’ the L^p spaces from the properties of T restricted to L^p spaces ‘at the endpoints’. On an informal level, suppose V and W are vector subspaces of measurable functions. A mapping $T : V \rightarrow W$ is said to be (p, q) -stable if $L^p \subseteq V$, $L^q \subseteq W$ and $T(L^p) \subseteq L^q$; and we say that T is (p, q) -stable and bounded whenever T restricts to a continuous mapping from L^p into L^q . The statement of Riesz-Thorin interpolation theorem (Theorem 9), is as follows.

Given a linear mapping $T : V \rightarrow W$ that is (p_j, q_j) -stable and bounded for $j = 0, 1$; then T is (p_t, q_t) -stable and bounded for all p_t, q_t whose reciprocals fall on the line segment in the *Riesz diagram* in Figure 1.

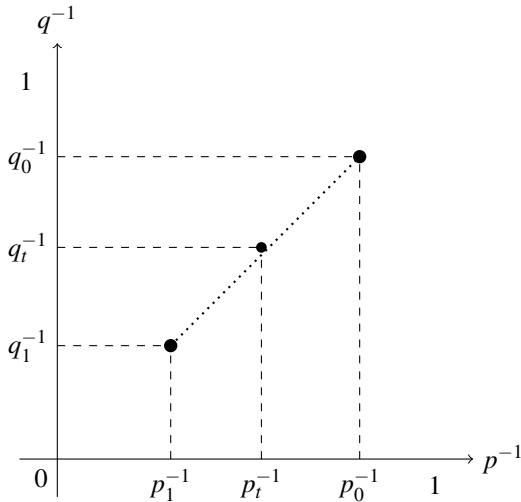


Figure 1: Points of the diagram represent the corresponding pair of reciprocals (p, q) , for which T is (p, q) -stable and bounded.

Given the technical nature of the proof of the interpolation theorem and the number of prerequisites involved, we have chosen to present the notation that we have chosen to use and a collection of definitions, and

needed results in Section 1. In particular, a special version of [1, Thm 2.10a,b] will be needed in the proof of the main result, as Folland omitted the case where $p_1 = \infty$, so Lemma 3 is written to address this gap. Next, we introduce an elementary ‘norming’ result in Theorem 6 that allows one to deduce embeddings of locally integrable functions into L^q spaces through the scalar product on essentially bounded functions with finite measure-theoretical support. Our presentation of Theorem 6 is non-standard, and the assertions made in Theorem 6, namely Statements (i) and (ii), loosely correspond to Theorems 6.13, and 6.14 in [1] respectively. The Three Lines Lemma, Lemma 8, is also introduced in Section 1.

1 PRELIMINARIES

Notation and Measure Theory

Let $\mathbb{N} = \{0, 1, 2, \dots\}$ denote the set of natural numbers (which includes 0), let $\mathbb{N}^+ = \{1, 2, \dots\}$ denote the set of counting numbers, let $\mathbb{Z} = \{0, -1, 1, \dots\}$ denote the set of integers, let \mathbb{R} denote the set of real numbers, and let \mathbb{C} denote the set of complex numbers. For any complex number $z \in \mathbb{C}$, its real and imaginary parts are denoted by $\text{Re}(z)$ and $\text{Im}(z)$ respectively. We also write

$$\text{sgn}(z) = \begin{cases} 0, & \text{if } z = 0 \\ z/|z|, & \text{if } z \neq 0 \end{cases}$$

and $\arg z \in (-\pi, \pi]$ for the argument of z . Assume that X and Y are normed vector spaces over \mathbb{C} . We denote by $\mathcal{L}(X, Y)$ the space of all linear maps from X to Y , by $L(X, Y)$ the space of all continuous linear maps from X to Y , and by X^* the continuous dual of X . Let (X, \mathcal{M}) be a measurable space, and denote by $\mathcal{E}(\mathcal{M})$ the collection of all complex-valued measurable functions on X .

Unless otherwise stated, sequences will be indexed by \mathbb{N}^+ and assumed to take values in a vector space. A sequence $\{x_n\}_{n=1}^\infty$ is said to be *finitely supported* if there exists an index N such that $x_n = 0$ for all $n > N$. We denote by l_0 the set of all finitely supported sequences, by c_0 the set of sequences that converge to 0 (whenever the codomain is equipped with a topology), by l^+

the set of all real-valued sequences with nonnegative terms, and by l^{++} the set of all real-valued sequences with strictly positive terms.

Let μ be a measure on \mathcal{M} . We denote by $\Sigma(\mu)$ the vector space of all simple functions, and by $\Sigma_0(\mu)$ the subspace of those simple functions that vanish outside a μ -finite set; that is,

$$\Sigma_0(\mu) = \{\phi \in \Sigma(\mu), \mu(\{x \in X : \phi(x) \neq 0\}) < \infty\}$$

The Banach space $L^\infty(\mu)$ consists of all essentially bounded functions, with the norm

$$\|f\|_\infty = \inf\{a \geq 0 : \mu(\{x \in X : |f(x)| > a\}) = 0\} \\ \forall f \in L^\infty(\mu)$$

We also denote by $L_0^\infty(\mu)$ the subspace of $L^\infty(\mu)$ consisting of functions that vanish outside a μ -finite set. Moreover, we let $L^+(\mu)$ denote the collection of measurable functions with values in $[0, \infty]$ (where $[0, \infty]$ is equipped with the extended Borel σ -algebra; see, for example, [1, Chap 2.1, 2.2, Ex 2.1, 2.2, 2.4]). We define $\Sigma^+(\mu)$ and $\Sigma_0^+(\mu)$ as the positive cones of $\Sigma(\mu)$ and $\Sigma_0(\mu)$, respectively; that is, these consist of the functions in $\Sigma(\mu)$ and $\Sigma_0(\mu)$ that take values in $[0, \infty)$. Recall that if $g \in L^+(\mu)$, its integral with respect to μ is defined as the supremum of the integrals of all nonnegative simple functions bounded above by g :

$$\int_X g(x)\mu(dx) = \sup \left\{ \int_X \phi(x)\mu(dx) : \phi \leq g, \phi \in \Sigma^+(\mu) \right\}$$

Moreover, if either μ is σ -finite or the support of g , namely $\{x \in X : g(x) \neq 0\}$, is σ -finite, then we may restrict the supremum to functions in $\Sigma_0^+(\mu)$; that is,

$$\int_X g(x)\mu(dx) = \sup \left\{ \int_X \phi(x)\mu(dx) : \phi \leq g, \phi \in \Sigma_0^+(\mu) \right\}$$

Lemma 1 ([1, Thm 2.10]). *Let (X, \mathcal{M}) be a measurable space, if $g : X \rightarrow \mathbb{C}$ is measurable, there exists a sequence of simple functions $\{\phi_n\} \subseteq \Sigma$, such that*

1. $\phi_n \rightarrow g$ pointwise,
2. $|\phi_n| \nearrow |g|$ pointwise.
3. If μ is σ -finite, or $\mu(\{|f| > \varepsilon\}) < \infty$ for all ε , we can take $\{\phi_n\} \subseteq \Sigma_0$.

Any sequence satisfying the first two conditions in Lemma 1 is called an *increasing sequence of subordinates* of g ; furthermore, if $\{f_n\}$ is any such sequence, then

$$\int_X |f_n(x)|\mu(dx) \nearrow \int_X |g(x)|\mu(dx)$$

Let p be a number in the interval $[1, \infty)$. We define

$$\mathcal{L}^p(\mu) = \left\{ f \in \mathcal{E}, (\mathcal{M}) \int_X |f(x)|^p \mu(dx) < \infty \right\}$$

and we denote by

$$L^p(\mu) = \mathcal{L}^p(\mu)/(\text{equality almost everywhere})$$

the corresponding quotient space. For any function f in either $\mathcal{L}^p(\mu)$ or $L^p(\mu)$, we define its L^p -norm by

$$\|f\|_p = \left(\int_X |f(x)|^p \mu(dx) \right)^{1/p}$$

It is well-known that $L^p(\mu)$ is a Banach space for every $p \in [1, \infty]$. A sequence $\{f_n\} \subseteq \mathcal{E}(\mathcal{M})$ is said to *converge in measure* to $f \in \mathcal{E}(\mathcal{M})$ if for every ε and $\delta > 0$, there exists $N \in \mathbb{N}^+$ such that

$$\mu(\{x \in X, |f_n(x) - f(x)| > \varepsilon\}) \leq \delta \quad \text{whenever } n \geq N$$

Definition ([1, p.25]). *A measure μ on \mathcal{M} is semifinite if every μ -infinite set E admits a measurable subset F such that $0 < \mu(F) < \infty$.*

Lemma 2 ([1, Ex 1.14]). *If μ is a semifinite measure, then for every $E \in \mathcal{M}$,*

$$\mu(E) = \sup\{\mu(F) < \infty, F \subseteq E, F \in \mathcal{M}\} \quad (1)$$

We recall that $\|f_n - f\|_\infty \rightarrow 0$ if and only if for every $\varepsilon > 0$,

$$\{\mu(\{|f_n - f| > \varepsilon\})\}_1^\infty \in l_0$$

Definition. *Let $f_n, f \in \mathcal{E}(\mathcal{M})$, we say that $f_n \rightarrow f$ in measure if for every $\varepsilon > 0$, the sequence formed by the numbers $\mu(\{|f_n - f| > \varepsilon\})$ is in l_0 .*

Lemma 3. *Let $1 \leq p_0 < p_t < p_1 \leq \infty$, and $f \in L^{p_t}$. There exists a decomposition $f = f_0 + f_1 \in L^{p_0} + L^{p_1}$, and a sequence $\{\phi_n\} \subseteq \Sigma_0$, such that $\phi_n = \phi_{n0} + \phi_{n1} \in \Sigma_0 + \Sigma_0$. This sequence satisfies*

1. $\phi_n \rightarrow f$ pointwise a.e., $\phi_{nj} \rightarrow f_j$ pointwise a.e. ($j = 0, 1$),
2. $|\phi_n| \nearrow |f|$ pointwise a.e., $|\phi_{nj}| \nearrow |f_j|$ pointwise a.e. ($j = 0, 1$),
3. $\|\phi_n - f\|_{p_t} \rightarrow 0$, and $\|\phi_{nj} - f_j\|_{p_j} \rightarrow 0$ ($j = 0, 1$).

Proof. By splitting $f = \sum_0^3 i^p f_p$ for $f_p \in L^+ \cap L^{p_t}(\mu)$ for $p = 0, \dots, 3$, we can assume that $f \geq 0$. Let ϕ_n be as in [1, Thm 2.10a,b], meaning

$$\phi_n = \sum_{k \in \mathbb{Z}} k 2^{-n} \chi_{E_n^k} + 2^n \chi_{F_n} \quad (2)$$

where $E_n^k = \{x \in X, f(x) \in (k 2^{-n}, (k+1) 2^{-n}]\}$, and $F_n = \{x \in X, f(x) > 2^n\}$. Since $f \in L^{p_t}$, we can use the same technique as in [1, Thm 6.9] in order to decompose $f = \chi_A f + (1 - \chi_A) f = f_0 + f_1$, where $A = \{x \in X, f > 1\}$. It follows that $f_j \in L^{p_j}$ for $j = 0, 1$.

Performing the same decomposition on the sequence of simple subordinates of f gives

$$\phi_n = \chi_A \phi_n + (1 - \chi_A) \phi_n = \phi_{n0} + \phi_{n1}$$

Properties (1-2) in the lemma are satisfied. As for Property (3), if $p_0 < p_t < p_1 < \infty$ then the result follows from the monotone convergence theorem. However if $p_1 = \infty$, then [1, Thm 2.10c] states that ϕ_{n1} converges essentially uniformly to f_1 as $n \rightarrow \infty$, and the proof is complete. \square

Theorem 4. Let $f_n, f, g : X \rightarrow \mathbb{C}$ be measurable functions.

1. For $p \in [1, \infty]$, if $\|f_n - f\|_p \rightarrow 0$, then $f_n \rightarrow f$ in measure (note that f_n, f are not necessarily in L^p)
2. If $f_n \rightarrow f$ in measure, then $f_{n_k} \rightarrow f$ a.e. for some subsequence
3. If $f_n \rightarrow f$ in measure, and $f_{n_j} \rightarrow g$ a.e. for some subsequence, then $f = g$ a.e.

Proof. The first claim follows from Chebyshev's inequality [1, Thm 6.17], the second and the third claims are proven in [1, Thm 2.30]. \square

1.1 Local Integrability

Definition. A measurable function $g : X \rightarrow \mathbb{C}$ is locally integrable if

$$\int_E |g(x)| dx < \infty \quad \text{for all } E \in \mathcal{M}, \mu(E) < \infty$$

The vector space of all locally integrable equivalence classes is denoted by $L^1_{loc}(\mu)$.

For $p \in [1, \infty]$ we consider $L^p(\mu)$ as a vector subspace of $L^1_{loc}(\mu)$, because for $p \in [1, \infty)$ and $g \in L^p(\mu)$ we have

$$\int_E |g(x)| dx \leq \int_E (|g(x)|^p + 1) \mu(dx) < \infty \quad (3)$$

On the other hand, if $p = \infty$, then $\int_E |g(x)| \mu(dx) \leq \|g\|_\infty \mu(E)$. Let $g \in L^1_{loc}$, consider the scalar product on L^∞_0

$$\langle g, f \rangle = \int_X g(x) f(x) dx \quad \forall f \in L^\infty_0 \quad (4)$$

The integral in Equation (4) converges absolutely, since

$$|g(x) f(x)| \leq \|f\|_\infty \chi_{\{f \neq 0\}} |g(x)| \in L^1.$$

Lemma 5 ([1, Ex 6.17]). If $g \in L^1_{loc}$, $q \in [1, \infty)$ and suppose that $M_q(g) = \sup\{|\langle g, f \rangle|, f \in L^\infty_0, \|f\|_p = 1\} < \infty$. Then,

1. for any $\varepsilon > 0$, $\mu(\{x \in X, |g(x)| > \varepsilon\}) < \infty$, and
2. $\text{supp } g = \{x \in X, |g(x)| \neq 0\}$ is σ -finite.

Proof of Lemma 5. If $\mu(\text{supp } g) < \infty$, both of the claims are immediate, so we are free to assume $\mu(\text{supp } g) = \infty$. For any $\varepsilon > 0$, let us write

$$A_\varepsilon = \{|g| > \varepsilon\}$$

The semifiniteness of μ (see Lemma 2) means that we can approximate $\mu(A_\varepsilon)$ by its subsets of finite measure.

$$\mu(A_\varepsilon) = \sup\{\mu(B), 0 < \mu(B) < \infty, B \subseteq A, B \in \mathcal{M}\}.$$

For any such B , we can make a clever choice of f that gives us a uniform upper bound on $\mu(B)$. Choose

$$f = (\overline{\text{sgn } g}) \chi_B \in L^\infty_0 \quad \text{which gives us} \quad (5)$$

$$\langle g, f \rangle = \int_B |g(x)| \mu(dx)$$

If $p \in [1, \infty)$ the relative largeness of f depends on $\mu(B)$, whereas if $p = \infty$, this 'largeness' equals 1:

$$\|f\|_p = \begin{cases} \mu(B)^{1/p} & p \in [1, \infty) \\ 1 & p = \infty \end{cases}$$

To obtain a lower bound for the integral on the right of Equation (5), notice that the simple function $\varepsilon \chi_A$ is a subordinate of $\chi_A |g|$. By the definition of the integral on L^+ , we see that

$$\varepsilon \mu(B) \leq \int_B |g(x)| \mu(dx) \leq \|f\|_p M_q(g).$$

Developing this further, we see that

$$\mu(B)^{1/q} \leq M_q^q(g) \varepsilon^{-q} \quad \forall q \in [1, \infty)$$

It follows upon taking the supremum over all such B , that

$$\mu(A_\varepsilon) \leq M_q^q(g) \varepsilon^{-q} < \infty \quad (6)$$

\square

Theorem 6 ([1, Thm 6.13, 6.14]). Given a locally integrable g , it is in L^q iff

$$M_q(g) = \sup\{|\langle g, f \rangle|, f \in L^\infty_0, \|f\|_p = 1\} < \infty, \quad (7)$$

where $p^{-1} + q^{-1} = 1$, and if this is the case, then $\|g\|_q = M_q(g)$.

Proof of Theorem 6. We can break up the proposition into two statements and prove them separately.

(i) If $g \in L^q$, then $M_q(g) \leq \|g\|_q$.

(ii) If $g \in L^1_{loc}$ and $M_q(g) < \infty$, then $g \in L^q$ and $\|g\|_q \leq M_q(g)$.

Statement (i) says that if $g \in L^q$, its scalar product on $\{f \in L_0^\infty, \|f\|_p = 1\}$ is uniformly bounded by its L^q norm. This follows from Hölder's inequality:

$$|\langle g, f \rangle| \leq \langle |g|, |f| \rangle \leq \|f\|_p \|g\|_q, \quad \text{for all } f \in L_0^\infty.$$

Hence **Statement (i)** is proven. We turn to the proof of **Statement (ii)**.

1. In the case where $q \in [1, \infty)$, let $\{\phi_n\} \subseteq \Sigma_0$ be an increasing sequence of subordinates of g (the existence of which is guaranteed using Lemma 1 and Lemma 5). Then,

$$\int |g(x)|^q \mu(dx) = \sup_n \int_X |\phi_n(x)|^q \mu(dx)$$

To show that $\|g\|_q \leq M_q(g)$, it suffices to prove $\liminf \|\phi_n\|_q \leq M_q(g)$. This is because the mapping $\varphi : t \mapsto t^{1/q}$ ($t \in [0, \infty]$, $q \in [1, \infty)$) satisfies $\sup \varphi(A) = \varphi(\sup(A))$ for all $A \subseteq [0, \infty]$. Hence,

$$\|\phi_n\|_q = \frac{\int_X |\phi_n(x)|^q \mu(dx)}{\|\phi_n\|_q^{q-1}} \quad (8)$$

For $n = 1, 2, \dots$, let us define

$$\psi_n(x) = \frac{|\phi_n(x)|^{q-1}}{\|\phi_n\|_q^{q-1}} (\overline{\text{sgn } g}) \in L_0^\infty \quad (9)$$

An easy calculation will show that $\|\psi_n\|_p = 1$. We can bound $\|\phi_n\|_q$ using the scalar product $\langle g, \psi_n \rangle$ (see Equation (8)) because each ϕ_n is a subordinate of g . This is accomplished by 'stealing' a factor of $|\phi_n(x)|$ under the integral sign.

$$\begin{aligned} \|\phi_n\|_q &= \frac{\int_X |\phi_n(x)|^q \mu(dx)}{\|\phi_n\|_q^{q-1}} \\ &\leq \frac{\int_X |\phi_n(x)|^{q-1} (\overline{\text{sgn } g}) g(x) \mu(dx)}{\|\phi_n\|_q^{q-1}} \\ &\leq M_q(g) \end{aligned}$$

2. If $q = \infty$, it is fruitful to consider an equivalent characterization of $\|g\|_\infty$.

$$\|g\|_\infty = \sup\{a \geq 0, \mu(\{x \in X, |g(x)| \geq a\}) > 0\} \quad (10)$$

If $\|g\|_\infty = 0$, then there is nothing to prove. So in the case that $\|g\|_\infty > 0$, we consider the lower approximants to $\|g\|_\infty$. Let $0 < \varepsilon < \|g\|_\infty$, the set $A_\varepsilon = \{|g| > \varepsilon\}$ must have positive measure (possibly ∞). Our measure μ is semifinite (see Equation (1)), so we find a measurable subset B of A with

$$0 < \mu(B) < \infty$$

We **note** that B is a subset of A_ε , so $|g(x)| \geq \varepsilon$ for a.e. $x \in B$. To show that $\varepsilon \leq M_q(g)$, we will evaluate g using the averaging operator

$$f_B = \mu(B)^{-1} \chi_B(\overline{\text{sgn } g})$$

It is easy to see that $f_B \in L_0^\infty$, and $\|f_B\|_1 = 1$. The scalar product of f_B with g gives the expression

$$\langle g, f_B \rangle = \frac{1}{\mu(B)} \int_B |g(x)| \mu(dx)$$

Our previous **note** tells us that $\varepsilon \leq \langle g, f_B \rangle \leq M_q(g)$ for all $\varepsilon < \|g\|_\infty$. Sending ε towards $\|g\|_\infty$ proves **Statement (ii)**. □

1.2 Rescaling between L^q and L^r spaces

Definition. Let $q, r \in [1, \infty]$, $q \neq \infty$, $f \in L^q$. If $f = |f|(\text{sgn } f)$ is the polar decomposition of f , we define

$$\tilde{f}_r = \begin{cases} |f|^{q/r} (\text{sgn } f) & r \neq \infty \\ \text{sgn } f & r = \infty \end{cases} \quad (11)$$

We offer a quick proof for the fact that \tilde{f}_r is in L^r , whose norm is determined by

$$\|\tilde{f}_r\|_r = \begin{cases} \|f\|_q^{q/r} & r \neq \infty \\ 1 \text{ or } 0 & r = \infty^1. \end{cases} \quad (12)$$

• If $r \neq \infty$, then $\|\cdot\|_r$ is computed directly using the integral

$$\|\tilde{f}_r\|_r^r = \int_X |f(x)|^{(q/r)r} \mu(dx) = \int_X |f(x)|^q = \|f\|_q^q$$

• If instead $r = \infty$, then $\|\text{sgn } f\|_\infty = 0$ iff $f = 0$ pointwise a.e, which proves Equation (12).

Theorem 7 ([1, Thm 6.10]). Let $1 \leq p_0 \leq p_1 \leq \infty$, fix $t \in [0, 1]$ and suppose $p_t \in [p_0, p_1]$ is given by

$$p_t^{-1} = (1-t)p_0^{-1} + (t)p_1^{-1} \quad (13)$$

Then, for all $f \in L^{p_0} \cap L^{p_1}$, its L^{p_t} norm can be estimated using the interpolation inequality

$$\|f\|_{p_t} \leq \|f\|_{p_0}^{(1-t)} \|f\|_{p_1}^t \quad (14)$$

Lemma 8 (Three Lines, [1, Thm 6.26]). Let φ be a bounded continuous function on $\text{Re}(z) \in [0, 1]$ that is holomorphic in $\text{Re}(z) \in (0, 1)$. If $|\varphi(z)| \leq M_0$ for $\text{Re}(z) = 0$ and $|\varphi(z)| \leq M_1$ for $\text{Re}(z) = 1$, then

$$|\varphi(z)| \leq M_0^{1-t} M_1^t$$

for any $t \in (0, 1)$, where $t = \text{Re}(z)$.

2 RIESZ-THORIN INTERPOLATION

Theorem 9 (Riesz-Thorin Interpolation, [1, Thm 6.27]). *Suppose that (X, \mathcal{M}, μ) and (Y, \mathcal{N}, ν) are positive, semifinite measure spaces. Let $1 \leq p_0, p_1, q_0, q_1 \leq \infty$, and constants $M_j \geq 0$ ($j = 0, 1$). Suppose we are given a linear mapping T*

$$T : (L^{p_0}(\mu) + L^{p_1}(\mu)) \rightarrow (L^{q_0}(\nu) + L^{q_1}(\nu))$$

which is (p_j, q_j) stable and bounded ($j = 0, 1$). That is, $T(L^{p_j}(\mu)) \subseteq L^{q_j}(\nu)$, and

$$\|Tf\|_{q_j} \leq M_j \|f\|_{p_j} \quad \text{for every } f \in L^{p_j}(\mu)$$

For any $t \in (0, 1)$, let p_t, q_t be exponents defined by the linear equations (or the Riesz diagram Figure 1)

$$\begin{aligned} p_t^{-1} &= (1-t)p_0^{-1} + (t)p_1^{-1} \\ q_t^{-1} &= (1-t)q_0^{-1} + (t)q_1^{-1} \end{aligned}$$

Then, T is (p_t, q_t) stable and bounded, and $\|Tf\|_{q_t} \leq M_t \|f\|_{p_t}$ for every $f \in L^{p_t}(\mu)$ where $M_t = M_0^{(1-t)} M_1^t$.

Proof. Let us consider this problem in the abstract for a little while. By convention, if $p = \infty$, then we write $p^{-1} = 0$. It will prove to be useful to define the exponents r_0, r_1 and r_t to be conjugate to q_0, q_1 and q_t . Using Figure 1, it is easy to see that

$$r_t^{-1} = (1-t)r_0^{-1} + (t)r_1^{-1} \tag{15}$$

as the reciprocals of Holder conjugates are reflections across 2^{-1} on the Riesz diagram. The linear equation that defines p_t^{-1} shows that p_t^{-1} is in the strict interior of a line segment with endpoints p_0^{-1} and p_1^{-1} . Since the extreme points² of $[0, 1]$ are $\{0, 1\}$. From which we deduce

$$\begin{aligned} p_t^{-1} \in \{0, 1\} &\text{ iff } p_0^{-1} = p_t^{-1} = p_1^{-1} \\ r_t^{-1} \in \{0, 1\} &\text{ iff } q_0^{-1} = q_t^{-1} = q_1^{-1} \in \{0, 1\} \end{aligned}$$

The reader should verify with Equation (15), and refer to Figure 1. The core argument of the rest of the proof consists of using rescaling trick in Section 1.2 with the Three Lines Lemma (Lemma 8) to obtain a uniform estimate for $\|Tf\|_{q_t}$ where f ranges over a dense subset of L^{p_t} with bounded norm. More precisely, we will prove

$$\|Tf\|_{q_t} \leq M_t \|f\|_{p_t} \quad \forall f \in \Sigma_0, \|f\|_{p_t} = 1 \tag{16}$$

With this, we can define a continuous linear operator $S : L^{p_t} \rightarrow L^{q_t}$ that extends $T|_{\Sigma_0}$ by uniform continuity. This is accomplished as follows: given any $f \in L^{p_t}$, let

²The extreme points of a convex subset C in a vector space X are the set of points $p \in C$ such that $(1-t)x + (t)y \neq p$ for all $x, y \in X$ and $t \in (0, 1)$.

$\{\phi_n\} \subseteq \Sigma_0$ converge to f in L^{p_t} , and $S(f)$ be the element such that

$$\|S(f) - T(\phi_n)\|_{q_t} \rightarrow 0 \tag{17}$$

This uniquely characterizes $S(f)$, because bounded linear operators such as $T|_{\Sigma_0}$ map Cauchy sequences to Cauchy sequences. A similar argument also shows that

$$\|S(f)\|_{q_t} \leq M_t \|f\|_{p_t} \quad \text{for every } f \in L^{p_t}. \tag{18}$$

Postponing the proof for the estimate in Equation (16) for the moment, let us verify that $S = T$ in the case where

$$1 \leq p_0 < p_t < p_1 \leq \infty \tag{19}$$

For any $f \in L^{p_t}$, we would like to make a special choice of ϕ_n that will be useful in some of the computations later on. The key idea is that we can improve the convergence properties of $\phi_n \rightarrow f$ if (1) we take our lower approximants from a smaller class of functions, and (2) we pass to a suitable subsequence.

Lemma 3, which we will restate for the convenience of the reader, gives us an approximation of f in L^{p_t} that also ‘splits’ in $L^{p_t} \subseteq L^{p_0} + L^{p_1}$.

For all $f \in L^{p_t}$, there exists a decomposition $f = f_0 + f_1 \in L^{p_0} + L^{p_1}$, and a sequence $\{\phi_n\} \subseteq \Sigma_0$, such that $\phi_n = \phi_{n0} + \phi_{n1} \in \Sigma_0 + \Sigma_0$. This sequence satisfies

1. $\phi_n \rightarrow f$ pointwise a.e., $\phi_{nj} \rightarrow f_j$ pointwise a.e ($j = 0, 1$),
2. $|\phi_n| \nearrow |f|$ pointwise a.e., $|\phi_{nj}| \nearrow |f_j|$ pointwise a.e. ($j = 0, 1$),
3. $\|\phi_n - f\|_{p_t} \rightarrow 0$, and $\|\phi_{nj} - f_j\|_{p_j} \rightarrow 0$ ($j = 0, 1$).

By passing to a subsequence of ϕ_n , we can use the properties of T to our advantage. For $j = 0, 1$,

$$\|T(\phi_{nj}) - T(f_j)\|_{q_j} \leq M_j \|\phi_{nj} - f_j\|_{p_j}$$

Convergence in norm ($1 \leq q_j \leq \infty$) means that we can relabel our sequence ϕ_{nj} and assume that $T(\phi_{nj}) \rightarrow T(f_j)$ pointwise a.e. (This comes from Theorem 4 for those that are unaware). Adding the two pieces together $T(\phi_{n0}) + T(\phi_{n1})$ gives us $T(\phi_n) \rightarrow T(f)$ pointwise a.e., as f is in the domain of T .

Since $1 \leq q_t \leq \infty$, and $\|S(f) - T(\phi_n)\|_{q_t} \rightarrow 0$, the sequence $\{T(\phi_n)\}$ of \mathcal{N} -measurable functions converges in measure to $S(f)$. One thinks of $S(f)$ as the best possible representative of the sequence of measurable functions $\{T(\phi_n)\}$. By a.e. uniqueness of this representative (proven in Theorem 4), we get $S(f) = T(f)$

pointwise a.e. Note that we cannot use positive definiteness of q_0 , q_1 , and q_t norms because the three sequences $T(\phi_n)$, $T(\phi_{n_0})$, and $T(\phi_{n_1})$ have limits that lie in three different L^q spaces. This proves that S is an extension of T under the assumption in Equation (19).

We now tackle the **estimate** Equation (16) (with the assumption $1 \leq p_0 < p_t < p_1 \leq \infty$ still in place). Given $f \in \Sigma_0$, with $\|f\|_{p_t} = 1$, the norm $\|Tf\|_{q_t}$ can be estimated by looking at the relative largeness of the scalar product (proven in Theorem 6)

$$\langle Tf, \cdot \rangle : L_0^\infty \rightarrow \mathbb{C}$$

Write $f = (\text{sgn } f) \sum |c_j| \chi_{E_j}$. For any $z \in [1, \infty]$, the rescaled version of f as in Section 1.2, is given by

$$\tilde{f}_z = \begin{cases} (\text{sgn } f) \sum |c_j|^{p_t/z} \chi_{E_j} & z \neq \infty \\ \text{sgn } f & z = \infty \end{cases}$$

We further subdivide the condition Equation (19) into two cases. The reasoning for this is because of the hypothesis of the rescaling trick.

1. If $q_0 = q_1$, to compute $\|Tf\|_{q_t}$, we fix an arbitrary $g \in L_0^\infty(\nu)$, with $\|g\|_{r_t} = 1$. The linearity of T and the evaluation map $\langle g, \cdot \rangle$ allows us to separate the effects of the rescaling from the action of g on $T(\chi_{E_j})$. For any $z \neq \infty$,

$$\begin{aligned} \langle g, T(\tilde{f}_z) \rangle &= \int_Y g(y) T(\tilde{f}_z)(y) \, dy \\ &= \sum |c_j|^{p_t/z} e^{i \arg c_j} \langle g, T(\chi_{E_j}) \rangle \end{aligned} \quad (20)$$

If $z = \infty$, a formula similar to Equation (20) can be obtained.

2. If $q_0 \neq q_1$, then $q_t^{-1} \notin \{0, 1\}$. Which rules out the possibility that $r_t = \infty$. For any $g \in \Sigma_0$, $\|g\|_{q_t} = 1$, suppose that $g = \sum |d_k| e^{i \arg d_k} \chi_{F_k}$. We can use the rescaling trick on both sides. Writing $\tilde{g}_z = |g|^{r_t/z} (\text{sgn } g)$, we see that for any $z \neq \infty$,

$$\begin{aligned} \langle \tilde{g}_z, T(\tilde{f}_z) \rangle &= \int_Y \tilde{g}_z(y) T(\tilde{f}_z)(y) \, dy \\ &= \sum |d_k|^{r_t/z} |c_j|^{p_t/z} e^{i(\arg c_j + \arg d_k)} \langle \chi_{F_k}, T(\chi_{E_j}) \rangle \end{aligned} \quad (21)$$

The sum in Equation (21) is over finitely many j, k . A similar equation is obtained if $z = \infty$.

In either case, with $g \in L_0^\infty$, or $g \in \Sigma_0$ held fixed, we will show that the scalar product is bounded by M_t . In symbols this means,

$$\begin{cases} |\langle g, T(\tilde{f}_{p_t}) \rangle| \leq M_t & q_0 = q_1 \\ |\langle \tilde{g}_{r_t}, T(\tilde{f}_{p_t}) \rangle| \leq M_t & q_0 \neq q_1 \end{cases} \quad (22)$$

The important part of Equations (20) and (21) is in the exponents, i.e. $|c_j|^{p_t/z}$ (resp. $|c_j|^{p_t/z} |d_k|^{r_t/z}$). It is also

useful to remember that $\tilde{f}_{p_t} = f$, and $\tilde{g}_{r_t} = g$ whenever $r_t \neq \infty$, as the exponent cancels out nicely. For any $\omega \in \mathbb{C}$, we define the function $\varphi : \mathbb{C} \rightarrow \mathbb{C}$,

$$\varphi(\omega) = \begin{cases} \langle g, T(\tilde{f}_{(1-\omega)p_0^{-1} + (\omega)p_1^{-1}}) \rangle & q_0 = q_1 \\ \begin{cases} \langle \tilde{g}_{(1-\omega)r_0^{-1} + (\omega)r_1^{-1}}, \\ T(\tilde{f}_{(1-\omega)p_0^{-1} + (\omega)p_1^{-1}}) \rangle \end{cases} & q_0 \neq q_1 \end{cases} \quad (23)$$

In both cases, $\varphi : \mathbb{C} \rightarrow \mathbb{C}$ is a holomorphic function because of ω placed in the exponent. Furthermore, if $\text{Re}\{\omega\} \in \{0, 1\}$, the relative sizes of the functions

$$\tilde{g}_{(1-\omega)r_0^{-1} + (\omega)r_1^{-1}} \quad \text{and} \quad \tilde{f}_{(1-\omega)p_0^{-1} + (\omega)p_1^{-1}}$$

remain unchanged as we perturb ω by a purely imaginary number. That is to say, suppose that $\text{Re}\{\omega\} = j \in \{0, 1\}$, then

$$\|\tilde{f}_{(1-\omega)p_0^{-1} + (\omega)p_1^{-1}}\|_{p_j} = \|\tilde{f}_{p_j}\|_{p_j} = 1, \text{ and} \quad (24)$$

$$\|\tilde{g}_{(1-\omega)r_0^{-1} + (\omega)r_1^{-1}}\|_{r_j} = \|\tilde{g}_{r_j}\|_{r_j} = 1 \quad (25)$$

By considering the cases where $\text{Re}\{\omega\} = j$ and $\text{Im}\{\omega\} = 0$, we obtain

$$\begin{cases} |\langle g, T(\tilde{f}_{p_j}) \rangle| \leq M_j & q_0 = q_1 \\ |\langle \tilde{g}_{r_j}, T(\tilde{f}_{p_j}) \rangle| \leq M_j & q_0 \neq q_1. \end{cases}$$

If $\text{Re}\{\omega\} = j \in \{0, 1\}$, and $\text{Im}\{\omega\} \neq 0$. We can use the ‘norm-invariance’ (as in Equation (24)) and see that $|\varphi(\omega)| \leq M_j$. By Lemma 8, this gives us an estimate for $\varphi(t)$

$$|\varphi(t)| \leq M_0^{(1-t)} M_1^{(t)} = M_t$$

where t has the same meaning as before, ($t \in (0, 1)$). In both subcases of $1 \leq p_0 < p_t < p_1 \leq \infty$, we conclude either directly or by a density argument of $\Sigma_0(\nu) \subseteq L_0^\infty(\nu)$, that the number

$$\|Tf\|_{q_t} = \sup\{|\langle g, Tf \rangle|, g \in L_0^\infty(\nu), \|g\|_{r_t} = 1\}$$

is bounded above by M_t . Since the simple function f is chosen arbitrarily, this completes the proof for the **estimate** under the assumption $1 \leq p_0 < p_t < p_1 \leq \infty$.

Let us tackle the remaining cases. If $p_0 \neq p_1$, we can always relabel the exponents such that $1 \leq p_0 < p_t < p_1 \leq \infty$. It remains to prove the **estimate** when $p_0 = p_t = p_1$ (and q_0, q_1, q_t unconstrained). This is straightforward because we can apply the interpolation inequality (proven in Theorem 7). For any $f \in L^{p_t}$, the function Tf is in $L^{q_0} \cap L^{q_1}$, which means

$$\|Tf\|_{q_t} \leq \|Tf\|_{q_0}^{(1-t)} \|Tf\|_{q_1}^{(t)} \leq M_t \|f\|_{p_t}. \quad (26)$$

The extension argument (and the proof of $S = T$) is unnecessary because Equation (26) holds for every $f \in L^{p_t}$. Therefore T restricts to a (p_t, q_t) stable and bounded linear operator with operator norm $\|T\| \leq M_t$, and the proof of the interpolation theorem is complete. \square

REFERENCES

- [1] Gerald B. Folland. *Real Analysis: Modern Techniques and Their Applications*. John Wiley & Sons, June 2013.

BRAIN TEASER 1

Courtesy of Hussin Suleiman

Alice and Bob play a game in which they must alternate placing a coin on a large circular table, such that no two coins touch each other. Alice goes first. When a player is unable to place a coin on the table, they lose. Who has a winning strategy?

Solution on page 49

MODELLING BASEBALL EXIT VELOCITIES WITH BLOCK MAXIMA

Jules Lanari-Collard

Since the introduction of Statcast ball-tracking technology to Major League Baseball, much work has been done by analysts to understand the value and uses for these data. The speed at which batters hit the ball (known as exit velocity) is of interest for player evaluation and projection, whilst the most useful information lies in the upper quantiles of each player distribution. This report uses extreme value methods to model exit velocity data and derives a metric to summarise each player's exit velocity distribution, performing well in comparison to existing metrics.

1 INTRODUCTION

1.1 Process over Outcomes

Baseball is the second-most popular sport in the United States [1], and the average Major League Baseball (MLB) franchise is worth \$2.4 billion. Teams invest significant amounts on player wages every year, with the median projected payroll for 2025 being \$144 million, and some teams projected for over \$270 million [2]. Salaries are often disproportionately concentrated in a small number of high-value players; Shohei Ohtani signed the largest contract in sports history, \$700 million over 10 years, in 2024 [3], and Juan Soto recently broke that record with a \$765 million, 15 year contract with the New York Mets [4].

With the amounts of money involved, franchises employ dedicated analytics teams within their front offices to inform decisions and evaluate and project players. Having a good understanding of a player's current and future ability is not only important when signing them to a large free agent contract, but also when trying to identify undervalued players.

Since the introduction of Statcast technology to MLB in 2015, allowing high-resolution ball and player tracking every game, there has been a shift in perspective on player evaluation. The technology allows analysts to evaluate events with respect to the *process*, not just the results. Instead of considering a ball in play as a binary event, either resulting in a hit or an out, we can consider the *expected outcome* in a probabilistic sense, given various factors such as the launch speed and launch angle. Over the course of many seasons, the wealth of data generated with this perspective has enabled a better separation between a player's true talent and luck and random variance; parsing the signal from the noise.

¹wOBACON stands for *Weighted On-Base Average on CONtact*. We will not go into the details of its calculation, but the main takeaway is that it measures the value of the outcomes of balls in play. For example, hits and home runs are positive, whilst outs are 0.

1.2 The Importance of Exit Velocity

One such Statcast metric is launch speed (more commonly known as **exit velocity**), simply measuring the speed (in mph) at which the baseball travels immediately after being hit by the bat. On a player level this has helped to quantify player 'power'. The use of this metric is rather intuitive; harder hit balls are more likely to turn into hits and even home runs. Figure 1 demonstrates this effect, using wOBACON¹ as a measure for outcome value, demonstrating an interesting trend; balls in play under 75mph all perform similarly, but above 75mph there is a clear positive correlation between exit velocity (EV) and quality of outcome.

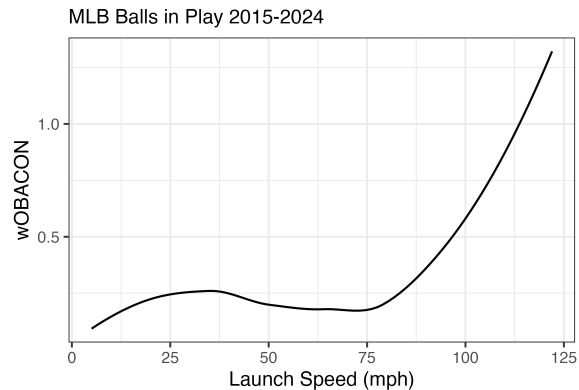


Figure 1: wOBACON and Exit Velocity

From the perspective of player evaluation, it follows that we can expect hitters who are able to consistently hit the ball harder to perform better. The question then turns to how can we best interpret each player's exit velocity data on a larger scale. To give an extreme example, suppose player A hits every ball at 100mph, whilst player B hits 80% of their batted balls at 95mph and the remaining 20% at 120mph. It is unclear which player provides more value; they have equal *average* exit velocities, but the value of their outcomes is not necessarily the same. Indeed, players across the league exhibit

very different exit velocity distributions, and designing metrics to describe these distributions is a topic of great debate. Figure 2 illustrates the difference in distribution shape between two highly contrasting players.

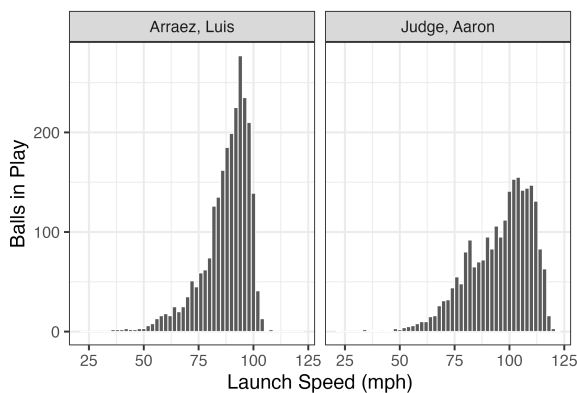


Figure 2: Comparison of Contrasting EV Distributions

1.3 Summarising Exit Velocity Data

Attempting to effectively summarise player-level exit velocity data, many metrics have already been formulated, with differing degrees of complexity. Before discussing the existing metrics, it is important to discuss what qualifies as an ‘informative’ or ‘useful’ metric. Metrics can be generally evaluated on three main criteria:

- Correlation with outcomes: how well does a metric represent value?
- Correlation with future outcomes: how well does a metric predict future outcomes and value?
- Variance: how much does a metric vary from year-to-year? In other words, how susceptible is the metric to random noise? In the search to separate true talent from randomness, low-variance (so-called ‘sticky’) metrics are much more reliable due to their robustness against random variation of the underlying data.

1.4 Existing Metrics

Average Exit Velocity

Self-explanatory in its definition, average EV is generally viewed as a flawed statistic, as it is equally affected by both the lower and upper quantiles of a player’s EV distribution. As seen in Figure 1, balls hit slower than 75mph should be viewed as roughly equal in value, and do not provide as much information as the upper quantiles.

²This was verified using an auto-correlation plot.

Best Speed

In response to the flaws of average EV, Tom Tango stated that we “learn nothing about a batter on their slow hit batted balls” [5], and instead proposed **best speed**, defined as the average of a batter’s top 50% hardest-hit balls. Best speed correlates better with outcomes and exhibits less year-to-year variation than average EV [6].

Exit Velocity Percentiles

Alternatively, one can consider the empirical quantiles of a player’s exit velocities. Commonly used quantiles are the 80th, 90th and 95th percentiles, known as **EV80**, **EV90** and **EV95** respectively [7]. They perform similarly to best speed in correlation with outcomes and predictive power, and are even lower variance than best speed.

Maximum Exit Velocity

Also self-explanatory, maximum EV is simply the maximum speed of a player’s hardest-hit ball over a given period of time, typically a season. Unsurprisingly, due to its inefficient use of information, it performs worse than the aforementioned metrics in correlation with outcomes, predictive power, and is only lower in variance than average EV.

1.5 Applying Extreme Value Theory

In summary, exit velocity data has a number of traits which render it difficult to analyse with traditional methods:

- EV distributions vary drastically from player to player, not only in parameters but also potentially in type of distribution.
- We learn very little about a player’s true talent from their slowly-hit batted balls (i.e. bottom 50%).
- Information about player talent lies in upper quantiles of their EV distribution.

Given that individual batted ball events (and thus also their block maxima) can safely be assumed to be i.i.d.², extreme value theory is particularly suited to this problem. Although player-level EV distributions may differ greatly, their block-maxima will follow a Generalised Extreme Value (GEV) distribution, allowing us to fit a model for each player without restrictive assumptions on their underlying EV distribution.

2 METHODS

2.1 Data

Data was collected using queries to the MLB Statcast Search API³, querying all balls in play from 2015 (implementation of Statcast tracking) to 2024. The full dataset consists of 1,157,634 batted ball events involving 2,373 unique hitters. 2,020 player seasons consisted of at least 250 batted ball events (BBEs), a threshold set to ensure sufficient sample size for good model fits in the ensuing analysis.

2.2 Block Maxima

Seeking to model the upper quantiles of each player's exit velocity distribution, we use the block-maxima method to fit a GEV model to the data. An alternative approach would be the Peaks-Over-Threshold (POT) method, however threshold selection is a complex problem, and not generalisable when looking to fit a model for each player. With the block-maxima method, we can set a constant block size for all models without overly adverse effects on the model fit.

The GEV parameters can be estimated using maximum likelihood methods with the `ismev` package [8] in *R*. Using only player seasons with at least 250 BBEs, a model was fitted for each player season (2,020 total) using a block size of 10 balls in play. The parameter of interest for evaluating the quality of the models is the shape (denoted ξ); MLE is not well-behaved for $\xi \in (-1, -\frac{1}{2}]$ and potentially unobtainable when $\xi \leq -1$. The software implementation did not encounter issues, although over 50% of the estimates had $\hat{\xi} \leq -\frac{1}{2}$, which is cause for concern.

When evaluating the fit of an individual GEV model, one can use visual diagnostic tools such as q-q plots and probability plots, however this becomes unfeasible when evaluating such a large number of models. Alternatively, we can use the well-known fact that the transform of a random sample drawn from a CDF F with F itself is standard uniformly distributed⁴. With this in mind, for each player season, we transform the block maxima by the GEV CDF with the estimated parameters. For a well-specified model, the resulting points should be approximately standard uniform, which we can test with the Kolmogorov-Smirnov Test for Uniformity. The p-values this test on each model are displayed in Figure 3, where we conclude that most of the transforms are in fact uniformly distributed at the 5% significance level.

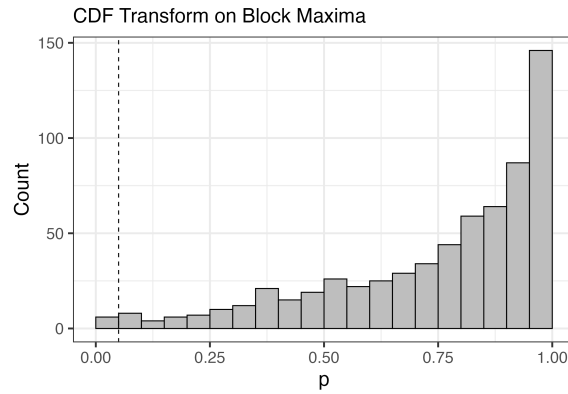


Figure 3: Evaluating Model Fit

2.3 Return Levels

A quantity of interest with the block maxima method is the **return level**. Usually interpreted in financial contexts, a k n -block return level represents the quantity one can expect to be exceeded once every k blocks of size n on average. For a GEV random variable with parameters μ, σ, ξ , the k n -block return level r can be computed using the following formula [9]:

$$r = \mu + \frac{\sigma}{\xi} \left[\left\{ -\ln \left(1 - \frac{1}{k} \right) \right\}^{-\xi} - 1 \right]$$

We can then estimate the return level by simply substituting in the parameter estimates. In this case return levels provide a useful, easy-to-understand statistic to interpret each player EV model. In particular, we can estimate a 5-block return level for each player, representing the EV we can expect them to exceed once every 50 balls in play (BIP), on average.

3 RESULTS AND DISCUSSION

3.1 Return Level as an EV Metric

We can now evaluate the quality of 50-BIP return levels as a metric for summarising each player's EV distribution, in particular with respect to the criteria described in section 1.3.

³Accessible at https://baseballsavant.mlb.com/statcast_search

⁴The inverse of this process is known as the inverse transform method, used for generating random samples from different distributions.

and the sample size required to achieve its demonstrated performance is relatively large. The choice of 10-BIP blocks and 5-block return levels was somewhat arbitrary, and improvements could be made by tuning those ‘parameters’. Although the metric performs relatively well across the whole sample, some individual models are extremely bad fits due to the estimated $\hat{\xi} < -1$ and non-uniformity of the CDF transform. One solution would be to simply filter out badly-specified models, however a metric which cannot be specified for certain players is definitely problematic. Bayesian inference for GEV models is an active area of research and could aid in the issue of $\hat{\xi} < -1$, by allowing for the imposition of constraints (in this case one could impose $\xi > -1$).

Another area for improvement would be the inclusion of covariates; age in particular. Methods exist for incorporating covariates in GEV models [9], however it is unclear how one could implement a general trend over many models. That is, although we fit a separate model for each player-season, an ageing trend is a population-wide effect, not player-specific. Such a problem is beyond the scope of this project, but nevertheless is an interesting area to explore.

3.3 Finite Upper Endpoints

A final point for discussion, unrelated to return levels, is to recall that a negative shape parameter bounds the GEV distribution from above. Given that almost all the models estimate a negative shape parameter, we can infer that each player has a *finite upper endpoint* to their EV distribution. This is an interesting if unsurprising result; we would expect there to be some physical limit to each player’s capabilities. Methods for the estimation of the upper endpoint are available [10], however the estimation is highly dependent on the shape parameter estimate. For ξ close to 0, the endpoint estimate becomes unreasonably high.

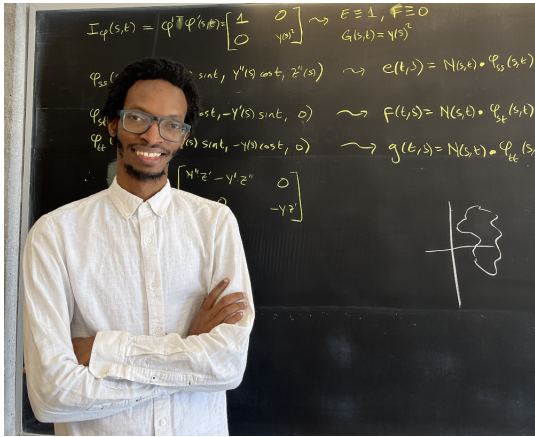
Estimating the upper endpoint for each player would be an alternative metric of interest; representing an estimate of their physical limits. However, when estimating the upper endpoint on the fitted player models, the estimates were indeed very unstable with the estimated shape parameter, and as a result don’t provide a useful interpretation.

REFERENCES

- [1] J. M. Jones. “Football retains dominant position as favorite u.s. sport.” (2023), [Online]. Available: <https://news.gallup.com/poll/610046/football-retains-dominant-position-favorite-sport.aspx> (visited on 11/23/2024).
- [2] Fangraphs. “Payroll breakdown, rosterresource.” (2024), [Online]. Available: <https://www.fangraphs.com/roster-resource/breakdowns/payroll> (visited on 11/23/2024).
- [3] S. Wexler. “\$700m stunner: Ohtani to dodgers on biggest deal in sports history.” (2023), [Online]. Available: <https://www.mlb.com/news/shohei-ohtani-contract-with-dodgers> (visited on 12/17/2024).
- [4] A. DiComo. “Mets, soto finalize record-breaking 15-yr, \$765m deal.” (2024), [Online]. Available: <https://www.mlb.com/news/juan-soto-a-grees-to-contract-with-mets> (visited on 12/17/2024).
- [5] T. Tango. “Statcast metric: Best speed.” (2022), [Online]. Available: <http://tangotiger.com/index.php/site/comments/statcast-metric-best-speed> (visited on 11/23/2024).
- [6] D. Andrews. “The doomed search for a perfect way to interpret exit velocity data.” (2023), [Online]. Available: <https://blogs.fangraphs.com/the-doomed-search-for-a-perfect-way-to-interpret-exit-velocity-data/> (visited on 11/23/2024).
- [7] B. Clemens. “You can’t fake exit velocity.” (2023), [Online]. Available: <https://blogs.fangraphs.com/you-cant-fake-exit-velocity/> (visited on 11/23/2024).
- [8] J. E. Heffernan and A. G. Stephenson., *Ismev: An introduction to statistical modeling of extreme values*, R package version 1.42, 2018. [Online]. Available: <https://CRAN.R-project.org/package=ismev>.
- [9] S. Coles, *An Introduction to Statistical Modeling of Extreme Values*. Springer, 2001.
- [10] I. F. Alves, P. Rosario, and C. Neves, “A general estimator for the right endpoint with an application to supercentenarian women’s records,” *Extremes*, 2016.

INTERVIEW WITH JEAN PIERRE MUTANGUHA

Helena Heinonen and Aahaan Rawal



$\delta\epsilon$: Could you tell me about your personal and academic background?

I'm from Rwanda, that's where I grew up and finished high school. I then did my undergrad at Oklahoma Christian University, where I finished in 2014. I did my grad school at University of Arkansas, finished 2020 right in the middle of the pandemic. After that, I've moved a bit: I was in Germany for a year, and then I was at Princeton for 3 years. Those were my post-doc positions and I just started my assistant professor position here.

$\delta\epsilon$: Why did you choose to study math?

I didn't know I wanted to do math in the beginning. Actually, I liked programming and did a lot of Project Euler, but some of the questions were actually a lot of math and I realized that I liked that much more than fighting with debugging code. When I started my undergrad, I wanted to do a double major math and computer science, but it would have taken 5 years. I knew I didn't want to do 5 years, so I chose math.

$\delta\epsilon$: Did you always know you wanted to be a professor?

No. I liked research, and it seemed like the only way to do research would be to be a professor. But then in my post-docs, when I had positions that were only research, I realized I didn't like that. I liked teaching as well because it gives structure to your day and something to do when you're stuck on your problem. It lets you say, "I taught something this week," every week. Whereas in research, you will have months where you just have nothing to show.

$\delta\epsilon$: What is your favourite part about Montreal?

I have not had the complete experience yet, but I saw

the tail end of the summer when I moved here in August: the festivals are really wonderful. Montreal is the first big city I've lived in since moving out of Rwanda. I grew up in Kigali, the capital city, which has about 2 million people. But after Kigali, all the other cities I moved to were small towns, like Princeton and Bonn. Princeton is a village. Bonn was nice, but it was still like maybe only 500,000. I enjoy taking the subway and not needing a car. But I'm not looking forward to shovelling snow.

$\delta\epsilon$: What is your favourite part about McGill?

So far I've enjoyed everyone I've worked with here. I've gotten a lot of support; you sort of need it when you start a position, and they've been wonderful. I also think that the department is doing good things for the students. There are a lot of opportunities for undergraduates and a culture of doing undergraduate research, which I never got to experience as an undergraduate: SURA in the summers, and independent readings people can do during the term. I think they are a great initiative. I'm looking forward to applying for a SURA to have undergraduate students this summer.

$\delta\epsilon$: Could you describe your current research?

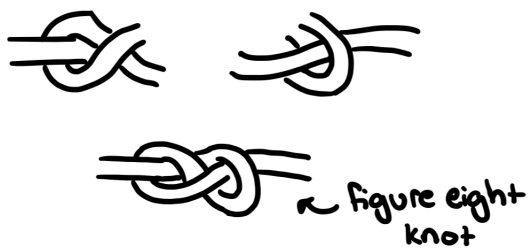
So my area is Geometric Group Theory, which I guess also explains why I like McGill and why I chose to come here in the first place: there's certainly a hub of geometric group theorists, so it's a very lively place to be in my field.

What is geometric group theory? When students maybe first learn what a group is in abstract algebra, they are studied very mechanically with formal symbols and axioms. Geometric group theory is the idea that you want to think of groups as symmetries of geometric objects, and how properties of your geometric objects end up translating to the properties of the group, and vice versa. If you know something about the group, you learn something about the geometric object you're interested in, and if you know something about the geometric object, you can learn something new about the group. That intersection of geometry and algebra is what I enjoy. That is the broad aspect of what I'm interested in.

$\delta\epsilon$: Do you have a favourite geometric object?

I like the figure eight knot. It turns out the exterior of the figure eight knot is an example of a mapping torus, one of these surface automorphisms that I'm interested in, and it's closely related to the automorphism of a free

group. But even though I'm calling it my favourite, I'm not that good at drawing it.



$\delta\epsilon$: How do you balance teaching, research, and mentoring graduate students effectively? What role do you think research plays in your development as a teacher?

I'm still figuring that out. I am still doing research, but it's sort of taking the back seat for now. In both of the terms that I have been here, I've been teaching a course for the first time, so I'm developing notes, problem sets, and midterms. I find that takes up most of my time. But everyone I talk to says your first year is kind of like that. Next year, when I get the same courses again, I will actually have time to balance the two.

So far I have taught courses that are closely related to the kind of things that I'm doing in my research. So my research kind of informs the types of questions I end up asking. For example, I'm teaching differential geometry, and the questions I ask on assignments or exams will be related to the things I'm interested in. I'm not just coming up with the questions, but I have to write the solutions too. So if there is a question I'm not interested in, writing the solutions will just be a headache. But this way I'm having fun with it.

$\delta\epsilon$: What are your favourite/least favourite parts about research?

With research, something you have to grapple with is being stuck. Any question or research problem that's worthwhile will probably not be immediate. You have to be willing to stick through it for a while. Now is this my least favourite part? I think it's just what you sign up for. But then whenever you figure it out, it's a fantastic feeling! You sort of stick through it so that you can get that satisfying feeling at the end once you answer the question.

Something I might say is one of my least favourite things would not be related to research itself, but the pressure and feeling like you have to produce something. It kind of takes away the fun. Sometimes it takes a while to get the results you want, but there's sort of

this pressure that you have to constantly produce something, every month, every 6 months, or every year - depending on your field.

$\delta\epsilon$: We found your math blog from your website, could you tell us a little more about that and its future visions?

Ah so you did some digging. Right, so how did it start? As an undergrad, at some point, I had wanted to learn things that your standard curriculum doesn't really expose you to, at least in the beginning of your undergraduate degree. But most of what I found online were either professors talking about the current research, which went way over my head, or they'd be sort of "popular blogs," like for the general public. These are still great, but there's only so much I could read about the Fibonacci sequence. So I said, okay assume I know some calculus, assume I know some number theory, but assume I'm not in grad school yet, what can I learn? But I couldn't really find anything like that. So I started my blog as an undergrad, also aimed at undergrads. But then grad school started and I got busy. I can see now why the thing I was hoping for doesn't quite exist because now, if I were to actively write, it would be more convenient to write about my research.

But since there are actually a lot of opportunities at McGill for undergraduate research, I think I could start writing about the projects that I work on with undergrads. So that is a potential future.

$\delta\epsilon$: What does the future hold for you? What are you excited about? Math or non-math related?

I'm excited to get through this winter season. If I can make it through, then I know I can survive the rest of my time here. I was told to actively take up winter activities, so I've been learning how to ice skate. And I'm excited to explore the city more.

Also, if I do get a chance to actually supervise undergraduate research this summer that would be really exciting. The project I'm proposing is related to differential geometry. I am curious about a different proof of the isoperimetric inequality which uses some interesting tools from partial differential equations.

$\delta\epsilon$: Do you have any advice for current undergrads?

Try to find things you enjoy, both math-wise but also in anything. There's a tendency for students to think: I want to get into this school, or this career, so I'm going to do the things that will get me there, like summer research. Not because I am interested in the research but because I think that is what is expected of me. But I think the right approach is really to find the things you enjoy in math and cultivate those. For example, if

you're going to work on a project, you're not just doing it because it will help you achieve whatever goals you have, but it will open you to exploring new ideas and help you figure out what you like. And sometimes the thing you think you like is not your favourite thing.

Consider your options, but make sure you're trying out things that you think will genuinely interest you. Don't apply for something that you're not interested in, it's a waste of your time.

9								4
	3			7		6	9	
		2	8					
	5							1
				4				3
8			7			4	5	
3					9			
							1	
	9			6		5	7	

JOKES _____

Call me a conspiracy theorist but π is not a circle! But why you may ask...

– Because πr^2

INERTIAL GRAVITY WAVE DERIVATION AND MODEL IMPLEMENTATION

Jelena Collins

This paper gives a basic overview of mountain gravity waves, then walks the reader through a derivation of a singular representative linear partial differential equation to calculate vertical wind perturbations. We begin with momentum, mass continuity, and adiabatic equations, and eventually define solutions to this equation in Fourier Space, which are implemented and analyzed with Python code.

1 INTRODUCTION

Gravity waves are the primary form of energy dispersion after stably stratified air is forced over topography like mountains or valleys. These mountain waves impact the direction and magnitude of flow above and around the mountain, and can have extending effects on zonal mean circulation near polar jet streams (Durran, 1990). Large amplitude waves can also impact aviation and cause extreme air gusts over lee sides of mountains. For my honours research thesis, I aimed to create a model to output the magnitude and direction of mountain gravity waves given parameters like initial wind speed, static stability, and topography.

The mathematical derivation begins with the Navier-Stokes momentum equation. From this, impacts from the Coriolis, centrifugal, and frictional forces were neglected due to the small scale, smooth topography, and general simplicity of my model. A constant horizontal wind was also applied, existing only in the x -direction, as the model is 2-dimensional in x and z . Finally, derivations were completed by assuming that each mathematical solution existed in a steady state. This is physically fairly accurate, but does not account for small perturbations in the steady-state.

The model itself is coded in Python. For each run, a Gaussian-style topography was assumed with shape depending on width and height. The model's outputs also were dependent on the Brunt-Väisälä frequency, and wind speed. Experiments were run to see the effect of each of these parameters on the steady-state wind.

2 LINEARIZATION OF FUNDAMENTAL EQUATIONS

2.1 Momentum Equation in x

The system of equations which represents fluid motion under the assumptions described above are derived from the momentum equations, as well as assumptions of incompressibility and an adiabatic atmosphere.

To derive the representative mountain wave equations, we begin with the momentum equation and focus on the x -term, u , in the \hat{i} direction. Implement the defini-

tion of the total derivative $\frac{D}{Dt}$, which includes a partial time derivative and an advecting gradient term. Note that \mathbf{u} here represents the applied wind vector, which is, in this case, $\langle u, 0, w \rangle$, as the model is two-dimensional in x and z . We also have the following parameters: air density ρ , pressure p , and gravitational acceleration g .

$$\begin{aligned}\frac{D\mathbf{u}}{Dt} &= -\frac{1}{\rho}\nabla p - g\hat{k} \\ \frac{D\mathbf{u}}{Dt} &= \frac{\partial u}{\partial t} + (\mathbf{u} \cdot \nabla)u = -\frac{1}{\rho}\frac{\partial p}{\partial x} - g\hat{k} \\ \frac{\partial u}{\partial t} + u\frac{\partial u}{\partial x} &= -\frac{1}{\rho}\frac{\partial p}{\partial x}\end{aligned}$$

To linearize each equation, parameters are split into appropriate mean-state and perturbation (prime) terms. The mean terms \bar{p} and $\bar{\rho}$ are functions of only z as these attributes vary predominantly in the z direction, while perturbations can exist in any dimension.

$$\begin{aligned}u &= U + u'(x, z, t) \\ w &= 0 + w'(x, z, t) \\ p &= \bar{p}(z) + p'(x, z, t) \\ \rho &= \bar{\rho}(z) + \rho'(x, z, t)\end{aligned}$$

Substitute these definitions into (2).

$$\frac{\partial(U + u')}{\partial t} + (U + u')\frac{\partial(U + u')}{\partial x} = -\frac{1}{\bar{\rho} + \rho'}\frac{\partial\bar{p} + p'}{\partial x}$$

However, for constant U and $\bar{p} = \bar{p}(x)$, non- z derivatives of these terms are 0. Additionally, since the magnitudes of perturbation terms are assumed $\ll 1$, we further linearize by approximating that products of perturbations are negligible. Finally, we use the Boussinesq approximation to define $\rho_0 = \bar{\rho} + \rho'$.

$$\begin{aligned}\frac{\partial u'}{\partial t} + (U + u')\frac{\partial u'}{\partial x} &= \frac{1}{\bar{\rho} + \rho'}\frac{\partial p'}{\partial x} \\ \rightarrow \frac{\partial u'}{\partial t} + U\frac{\partial u'}{\partial x} &= \frac{1}{\rho_0}\frac{\partial p'}{\partial x}\end{aligned}\quad (27)$$

2.2 Momentum Equation in z

Now, return to the momentum equation and focus on z -term, w , in the \hat{k} direction.

$$\frac{D\mathbf{u}}{Dt} = \frac{\partial w}{\partial t} + (\mathbf{u} \cdot \nabla)w = -\frac{1}{\rho}\frac{\partial p}{\partial z} - g\hat{k}$$

Separate mean and perturbation terms and neglect products of perturbations as in x .

$$\frac{\partial w'}{\partial t} + U \frac{\partial w'}{\partial x} = -\frac{1}{\bar{\rho} + \rho'} \frac{\partial \bar{p} + p'}{\partial z} - g \hat{k}$$

Implement the small-amplitude assumption in the equation above to reduce to

$$\frac{\partial w'}{\partial t} + U \frac{\partial w'}{\partial x} = -\frac{1}{\bar{\rho}} \left(1 - \frac{\rho'}{\bar{\rho}}\right) \left(\frac{\partial \bar{p}}{\partial z} + \frac{\partial \rho'}{\partial z}\right) - g \hat{k}$$

Assume hydrostatic balance to substitute $\frac{\partial \bar{p}}{\partial z} = -\bar{\rho} g \hat{k}$ and simplify by neglecting products of perturbations.

$$\frac{\partial w'}{\partial t} + U \frac{\partial w'}{\partial x} = -\left(\frac{1}{\bar{\rho}} \frac{\partial \rho'}{\partial z} + \frac{\rho' g}{\bar{\rho}}\right)$$

Use the Boussinesq approximation to substitute $-\rho'/\bar{\rho} \approx \theta'/\bar{\theta}$ and to set $\bar{\rho} = \rho_0$.

$$\frac{\partial w'}{\partial t} + U \frac{\partial w'}{\partial x} = -\frac{1}{\rho_0} \frac{\partial \rho'}{\partial z} + \frac{\theta' g}{\bar{\theta}}$$

Finally, use the definition of buoyancy, $b = \theta' g / \bar{\theta}$ to reach a final equation in z .

$$\frac{\partial w'}{\partial t} + U \frac{\partial w'}{\partial x} = -\frac{1}{\rho_0} \frac{\partial \rho'}{\partial z} + b \quad (28)$$

2.3 Adiabatic and Incompressibility Equations

Next, linearize the adiabatic equation by beginning with the equation representing an adiabatic atmosphere, in which potential temperature θ of a given parcel of air does not change in time.

$$\begin{aligned} \frac{D\theta}{Dt} &= \frac{\partial \theta}{\partial t} + (\mathbf{u} \cdot \nabla) \theta = 0 \\ \rightarrow \frac{\partial \theta}{\partial t} + (U + u') \frac{\partial \theta}{\partial x} + w' \frac{\partial \theta}{\partial z} &= 0 \end{aligned}$$

In a vertically stratified atmosphere, $\bar{\theta} = \bar{\theta}(z)$. Separate θ into mean and perturbation components as above, such that $\theta = \bar{\theta} + \theta'(x, z, t)$.

$$\begin{aligned} \frac{\partial(\bar{\theta} + \theta')}{\partial t} + U \frac{\partial(\bar{\theta} + \theta')}{\partial x} + u' \frac{\partial(\bar{\theta} + \theta')}{\partial x} \\ + w' \frac{\partial(\bar{\theta} + \theta')}{\partial z} = 0 \end{aligned}$$

As $\bar{\theta} = \bar{\theta}(z)$, set all non- z derivatives of $\bar{\theta} = 0$ and approximate all products of perturbation terms as 0.

$$\begin{aligned} \frac{\partial \theta'}{\partial t} + U \frac{\partial \theta'}{\partial x} + w' \frac{\partial \bar{\theta}}{\partial z} &= 0 \\ \rightarrow \frac{\partial \theta'}{\partial t} + U \frac{\partial \theta'}{\partial x} &= -w' \frac{\partial \bar{\theta}}{\partial z} \end{aligned}$$

Multiply each side by $g/\bar{\theta}$.

$$\frac{g}{\bar{\theta}} \frac{\partial \theta'}{\partial t} + U \frac{g}{\bar{\theta}} \frac{\partial \theta'}{\partial x} = -\frac{w' g}{\bar{\theta}} \frac{\partial \bar{\theta}}{\partial z}$$

Define static stability $N^2 = (g/\bar{\theta})(\partial \bar{\theta}/\partial z)$ and use the definition of buoyancy, $b = \theta' g / \bar{\theta}$, from above for the final form of the linearized adiabatic equation.

$$\frac{\partial b}{\partial t} + U \frac{\partial b}{\partial x} = -N^2 w' \quad (29)$$

Finally, linearize the incompressibility equation, which, under mass continuity, dictates that

$$\nabla \cdot \mathbf{u} = 0 \quad \rightarrow \quad \left\langle \frac{\partial}{\partial x}, \frac{\partial}{\partial y}, \frac{\partial}{\partial z} \right\rangle \cdot \langle u, v, w \rangle = 0$$

Substitute mean and perturbation terms as defined earlier and expand.

$$\frac{\partial(U + u')}{\partial x} + \frac{\partial w'}{\partial z} = 0$$

For constant U , this becomes

$$\frac{\partial u'}{\partial x} + \frac{\partial w'}{\partial z} = 0 \quad (30)$$

3 CREATION OF A SINGLE-VARIABLE EQUATION

3.1 Reduction to Two Equations

Equations (1)-(4) establish a system of partial differential equations to represent adiabatic, incompressible flow over a mountain. These equations are dependent on wind perturbations u' and w' ; dimensional variables x, z , and t ; and atmospheric variables and values ρ', ρ_0, b', U , and N^2 . Now, we seek to create a singular representative equation in w . To begin, reduce the system of four equations to two equations in w and p . To construct the first equation, combine (2) and (3) to eliminate the buoyancy term b by defining a linear advection operator $\mathcal{L} = \left(\frac{\partial}{\partial t} + U \frac{\partial}{\partial x}\right)$. Recognize that in the left side of (2),

$$\frac{\partial w'}{\partial t} + U \frac{\partial w'}{\partial x} = \left(\frac{\partial}{\partial t} + U \frac{\partial}{\partial x}\right) w' = \mathcal{L} w'$$

and in (4), that

$$\frac{\partial b}{\partial t} + U \frac{\partial b}{\partial x} = \left(\frac{\partial}{\partial t} + U \frac{\partial}{\partial x}\right) b = \mathcal{L} b$$

Rewrite these equations appropriately.

$$\mathcal{L} w' = -\frac{1}{\rho_0} \frac{\partial \rho'}{\partial z} + b \quad \mathcal{L} b = -N^2 w'$$

Apply the \mathcal{L} operator again to the left-hand equation to create a second $\mathcal{L}b$ term, and substitute this definition into the right-hand equation to eliminate the system's dependence on b .

$$\begin{aligned}\mathcal{L}^2 w' &= \mathcal{L} \left[-\frac{1}{\rho_0} \frac{\partial p'}{\partial z} \right] + \mathcal{L}b \\ \rightarrow \mathcal{L}b &= \mathcal{L}^2 w' - \mathcal{L} \left[-\frac{1}{\rho_0} \frac{\partial p'}{\partial z} \right] \\ \mathcal{L}^2 w' - \mathcal{L} \left[-\frac{1}{\rho_0} \frac{\partial p'}{\partial z} \right] &= -N^2 w'\end{aligned}\quad (5)$$

For the second equation in w and p , rewrite equation (1) with the linear operator above.

$$\frac{\partial u'}{\partial t} + U \frac{\partial u'}{\partial x} = \mathcal{L}u' = -\frac{1}{\rho_0} \frac{\partial p'}{\partial x}$$

Apply \mathcal{L} to the linearized mass continuity equation (4).

$$\mathcal{L} \frac{\partial u'}{\partial x} + \mathcal{L} \frac{\partial w'}{\partial z} = 0$$

Take the x derivative of the momentum equation in x to match the $\mathcal{L} \frac{\partial u'}{\partial x}$ term in the new mass continuity equation.

$$\mathcal{L}u' = -\frac{1}{\rho_0} \frac{\partial p'}{\partial x} \quad \rightarrow \quad \mathcal{L} \frac{\partial u'}{\partial x} = -\frac{1}{\rho_0} \frac{\partial^2 p'}{\partial x^2}$$

Substitute this definition into the mass continuity equation with the linear operator.

$$\begin{aligned}\mathcal{L} \frac{\partial u'}{\partial x} + \mathcal{L} \frac{\partial w'}{\partial z} &= 0 \\ \rightarrow -\frac{1}{\rho_0} \frac{\partial^2 p'}{\partial x^2} + \mathcal{L} \frac{\partial w'}{\partial z} &= 0 \\ \rightarrow \mathcal{L} \frac{\partial w'}{\partial z} &= \frac{1}{\rho_0} \frac{\partial^2 p'}{\partial x^2} \\ \rightarrow \rho_0 \mathcal{L} \frac{\partial w'}{\partial z} &= \frac{\partial^2 p'}{\partial x^2}\end{aligned}\quad (6)$$

3.2 Reduction to One Equation and Steady-State

Now, we have two equations in two variables, w' and p' . We seek to combine them to create a single governing equation in w . Begin by taking the z derivative of (6).

$$\begin{aligned}\frac{\partial}{\partial z} \left[\frac{\partial}{\partial z} \rho_0 \mathcal{L}w' \right] &= \frac{\partial}{\partial z} \left[\frac{\partial^2 p'}{\partial x^2} \right] \\ \rightarrow \frac{\partial^2}{\partial z^2} \rho_0 \mathcal{L}w' &= \frac{\partial^3 p'}{\partial x^2 \partial z}\end{aligned}$$

Then, apply \mathcal{L} to each side.

$$\frac{\partial^2}{\partial z^2} \rho_0 \mathcal{L}^2 w' = \mathcal{L} \frac{\partial^3 p'}{\partial x^2 \partial z}$$

Now, apply $\frac{\partial^2}{\partial x^2}$ to (5).

$$\frac{\partial^2}{\partial x^2} [-\rho_0 (\mathcal{L}^2 w' + N^2 w')] = \frac{\partial^2}{\partial x^2} \mathcal{L} \frac{\partial p'}{\partial z} = \mathcal{L} \frac{\partial^3 p'}{\partial x^2 \partial z}$$

Having set the right-hand side of each equation to $\mathcal{L} \frac{\partial^3 p'}{\partial x^2 \partial z}$, we can set the left-hand sides equal to each other to form a single equation in w .

$$\frac{\partial^2}{\partial z^2} \rho_0 \mathcal{L}^2 w' = \frac{\partial^2}{\partial x^2} [-\rho_0 (\mathcal{L}^2 w' + N^2 w')]$$

Divide each side by ρ_0 and move all terms to the same side, then distribute.

$$\begin{aligned}\frac{\partial^2}{\partial z^2} \mathcal{L}^2 w' + \frac{\partial^2}{\partial x^2} [(\mathcal{L}^2 w' + N^2 w')] &= 0 \\ \frac{\partial^2}{\partial z^2} \mathcal{L}^2 w' + \frac{\partial^2}{\partial x^2} \mathcal{L}^2 w' + \frac{\partial^2}{\partial x^2} N^2 w' &= 0\end{aligned}$$

Factor \mathcal{L} and replace with original advection operator $\left(\frac{\partial}{\partial t} + U \frac{\partial}{\partial x}\right)$ to reach the final version of the single-variable partial differential equation in w .

$$\mathcal{L}^2 \left(\frac{\partial^2 w'}{\partial z^2} + \frac{\partial^2 w'}{\partial x^2} \right) + \frac{\partial^2}{\partial x^2} N^2 w' = 0$$

$$\left(\frac{\partial}{\partial t} + U \frac{\partial}{\partial x} \right)^2 \left(\frac{\partial^2 w'}{\partial z^2} + \frac{\partial^2 w'}{\partial x^2} \right) + \frac{\partial^2}{\partial x^2} N^2 w' = 0 \quad (7)$$

Since our model aims to find the final form gravity waves over topography, we are seeking a solution which is not changing in time. We will adopt this by setting $\frac{\partial}{\partial t} = 0$ in (7).

$$U^2 \frac{\partial^2}{\partial x^2} \left(\frac{\partial^2 w'}{\partial z^2} + \frac{\partial^2 w'}{\partial x^2} \right) + N^2 \frac{\partial^2 w'}{\partial x^2} = 0$$

Use the Fundamental Theorem of Calculus to integrate.

$$\begin{aligned}\int U^2 \frac{\partial^2}{\partial x^2} \left(\frac{\partial^2 w'}{\partial z^2} + \frac{\partial^2 w'}{\partial x^2} \right) \partial^2 x &= - \int N^2 \frac{\partial^2 w'}{\partial x^2} \partial^2 x \\ U^2 \left(\frac{\partial^2 w'}{\partial z^2} + \frac{\partial^2 w'}{\partial x^2} \right) &= -N^2 w' \\ \rightarrow \frac{\partial^2 w'}{\partial z^2} + \frac{\partial^2 w'}{\partial x^2} &= -\frac{N^2}{U^2} w'\end{aligned}$$

Therefore, the linear, single-variable, two-dimensional, and steady-state form of our partial differential equation can be written as a function of variables x and z ,

$$\frac{\partial^2 w'}{\partial z^2} + \frac{\partial^2 w'}{\partial x^2} + \frac{N^2}{U^2} w' = 0 \quad (8)$$

4 NORMAL MODE SOLUTIONS AND MODEL IMPLEMENTATION

To find solutions to the equation above, we substitute a normal waveform solution $w(x, t) = ce^{i(kx+mt)}$. From this, $m = \pm\sqrt{\frac{N^2}{U^2} - k^2}$, and solutions can be broken into conditions where $m \in \mathbb{R}$ and $m \in \mathbb{C}$.

For $m \in \mathbb{C}$, we can define $c = \sqrt{k^2 - \frac{N^2}{U^2}}$ such that $m = \pm ic$. In this case, w can be written as the superposition of two waves, such that, for arbitrary parameters a and $b \in \mathbb{R}$,

$$w(x, z) = ae^{i(kx+mt)} + be^{i(kx-mz)}$$

To solve this equation, two boundary conditions must be implemented. We will approximate here that surface flow at $z = 0$ runs parallel to the terrain, $h(x)$, such that $w(x, 0) = U \frac{\partial h}{\partial x}$. Additionally, it is known that wave energy under these conditions dissipates such that $w(x, \infty) = 0$. With these two boundary conditions in place, we find that in Fourier space,

$$w(k, z) = ikU\hat{h}(k)e^{-\sqrt{k^2 - \frac{N^2}{U^2}}z} \quad k^2 > N^2/U^2 \quad (1)$$

For $m \in \mathbb{R}$, we use the same parallel surface boundary condition $w(x, 0) = U \frac{\partial h}{\partial x}$, but encounter propagation rather than decay of vertical waves at large heights. Therefore, for these solutions, we use a boundary condition which restricts to positive energy flux within the system. This simplifies to $wp'/\rho_0 > 0$ for energy flux $E = u^2 + w^2 + \frac{b^2}{N^2} > 0$. For these new boundary conditions, we find in Fourier Space that

$$w(k, z) = ikU\hat{h}(k)e^{iz\sqrt{\frac{N^2}{U^2} - k^2}} \quad k^2 < N^2/U^2, k > 0 \quad (2)$$

$$w(k, z) = ikU\hat{h}(k)e^{-iz\sqrt{\frac{N^2}{U^2} - k^2}} \quad k^2 < N^2/U^2, k < 0 \quad (3)$$

Results were gathered by implementing topographical Fourier-transformed topographical functions in k to these equations in Python and taking the inverse Fourier Transform of the results at each z level for parameterized N and U values.

For a model resolution of 256×256 , a Brunt-Väisälä frequency (N) of 0.1 Hz, and a constant wind speed U of 5 m/s, I defined a Gaussian topography with a width of 25 kilometers and a height of 500 meters. The results of this experiment can be seen in Figure 1.

However, note that the features of this plot and the waves' propagational intensity changes when parameters are varied. For instance, when the terrain's aspect ratio is increased, k increases. This increases the

value of k^2 , which then has an impact on $\sqrt{k^2 - \frac{N^2}{U^2}}$ and causes the wave to become less hydrostatic. These waves show evidence of decay, as seen below, where the wind magnitude is clearly significantly less than with the initial parameters. This can be seen in Figure 2.

Further experimentation showed that the Brunt-Väisälä frequency has the effect of increasing or decreasing the number of separate flow groups in a given direction. A greater Brunt-Väisälä frequency leads to more separate air layers travelling in different directions. The frequency has no effect on the magnitude of the flow. Additionally, as is intuitive, an increased constant westerly wind speed, U , leads to an increased wind speed within stratified layers.

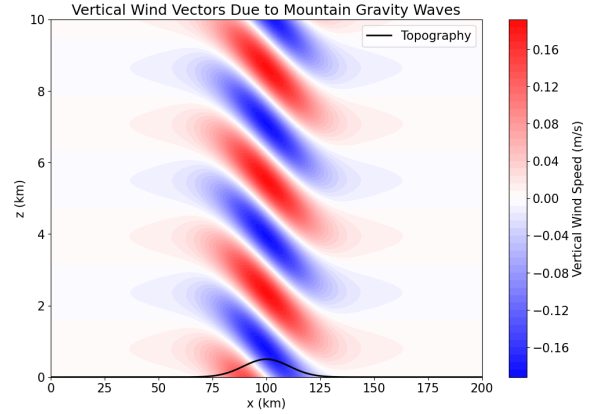


Figure 1: Contour plot of mountain gravity wave magnitude and directions with initial parameters as declared in code. Gaussian mountain width of 25000 m (25 km) and height of 500 m (0.5 km). Wind speed of 5 m/s, Brunt-Väisälä frequency of 0.01 s^{-1} .

Overall, the computer model behaves as mathematically expected. It shows an increase in w wind value with height; an increase in w wind value with an increase in mean horizontal wind; more layers and less tilt with a greater Brunt-Väisälä frequency; and wind in the opposite direction for inverted topography. It also shows maximal w wind along the surface and minimal w wind as one moves west beyond the topography.

The model does make many assumptions which affect its alignment with reality, such as neglecting friction and the Brunt-Väisälä frequency's height dependence. That said, preliminary results show the desired phenomena, and the model represents gravity waves at a spatial resolution currently unattainable by large-scale climate models.

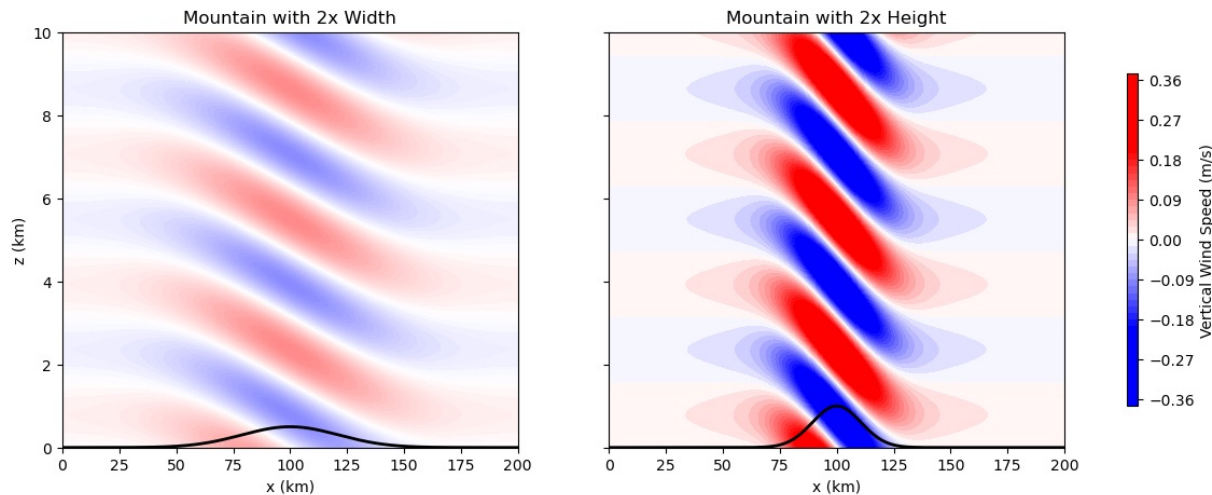


Figure 2: Contour plot of mountain gravity wave magnitude and directions with increased aspect ratio to decrease hydrostatic effect. The left image has a mountain with width 50 km and height of 0.5 km. The right image has a mountain with width 25 km and a height of 1 km. Each has a wind speed of 5 m/s and a Brunt-Väisälä frequency of 0.01 s^{-1} .

REFERENCES

- [1] Durran, D. R. (1990). Mountain waves and downslope winds. *Atmospheric Processes over Complex*

Terrain, 59-81. https://doi.org/10.1007/978-1-935704-25-6_4

BRAIN TEASER 2

Putnam 2008 A2

Alan and Barbara play a game in which they take turns filling in entries of an initially empty 2008×2008 array. Alan plays first. At each turn, a player chooses a real number and places it in a vacant entry. The game ends when all the entries are filled. Alan wins if the determinant of the resulting matrix is nonzero; Barbara wins if it is zero. Which player has a winning strategy?

Hint: Have you tried Brain Teaser 1 on page 7 yet? You might want to warm up with that one, then try a similar approach here...

Solution on page 49

FRACTAL GEOMETRY: THE EXPLORATION OF JULIA SETS

Gabriella Chen

This report explores the dynamics of Julia sets associated with the quadratic map $z_{n+1} = z_n^2 + c$, where c is a complex parameter. The focus is on the iterative properties, fixed points, stability analysis, and visualizations of Julia sets. Numerical simulations are conducted to reveal self-similar structures and the fractal nature of these sets.

1 INTRODUCTION

Fractals are intricate, endlessly complicated patterns. They are typically characterized as “a rough or fragmentary geometric shape that can be divided into several parts, with each part being (at least approximately) a reduced shape of the whole,” implying self-similarity. B.B. Mandelbrot coined the term “fractal” in 1975 [8] with his insights on the relation between theoretical discovery and geometric patterns in nature. Julia sets are distinct from other fractals as they are created through iterative processes in the complex plane that adhere to basic mathematical principles.

Julia sets are generated from the iterative function $z_{n+1} = z_n^2 + c$, where z and c are complex numbers. The behaviour of the iterates z_n depends on the value of c , as well as the initial condition z_0 . For certain values of c , the resulting Julia sets are connected, forming continuous and intricate patterns. For other values of c , the Julia sets are disconnected, forming a “dust” structure. This sensitivity to c links Julia sets closely to the Mandelbrot set, a well-known fractal that lives inside the space of parameters c .

Julia set theory is closely related to important concepts in nonlinear dynamics such as stability, chaos, and bifurcation. Fixed points and their stability as well as the divergent behavior of points in the complex plane are fundamental to understanding the dynamics of systems. Additionally, Julia sets provide a striking visualization of the transition between order and chaos.

This report focuses on the mathematical and visual exploration of Julia sets. The main objectives are:

1. To analyze the mathematical foundation underlying Julia sets, including their connection to fixed points and stability.
2. To investigate how the structure of Julia sets changes with different values of c , emphasizing the boundary between connected and disconnected sets, and also how to determine their connectivity mathematically.
3. To numerically simulate and visualize Julia sets for various values of the parameter c , highlighting their fractal and self-similar properties.

4. To provide insights into the fractal geometry and dynamical systems techniques that underlie the creation and analysis of Julia sets. In addition, to offer a brief explanation of the connection between Julia sets and Mandelbrot sets.

Through these explorations, the report aims to demonstrate the rich mathematical structures that emerge from simple iteration rules. In addition, it emphasizes the use of numerical methods and computational tools to study nonlinear dynamics problems.

2 MATHEMATICAL BACKGROUND

2.1 Formal Definitions of Julia Sets

The following definitions are adapted from 4.1 and 4.2 of [4].

Definition (Orbit). Given a set of complex quadratic polynomials $f_c : z \mapsto z^2 + c$, the orbit of $z_0 \in \mathbb{C}$ is the sequence z_0, z_1, z_2, \dots where $z_{n+1} = f_c(z_n)$.

Definition (Filled Julia set). For such complex quadratic polynomials $f_c : z \mapsto z^2 + c$, the filled Julia set, $K_c = \{z \in \mathbb{C} \mid \exists s \in \mathbb{R}, \forall n \in \mathbb{N}, |f_c^n(z)| \leq s\}$, where $f_c^n(z)$ is the n th iterate of $f_c(z)$. That is, for a given c , consider the orbit of every starting point. The set of all bounded orbits that do not escape to infinity forms a filled Julia set.

Definition (Julia set). The Julia set J_c is the set of points that constitutes the boundary of the filled Julia set K_c .

2.2 Connected and Totally Disconnected

We recall the following theorem based on Frame and Urry in their work of *Fractal Worlds* [6], specifically technical notes A.48, and present them in the special case of the function f_c .

Theorem 1 (Fatou-Julia Theorem). If the orbit of 0 escapes to infinity, J_c is a Cantor set, and if the orbit does not escape to infinity, J_c is connected.

Corollary 2 (Dichotomy Theorem). The Julia set J_c of $z^2 + c$ is either connected or totally disconnected (Cantor set).

Remark. The above result is derived from the previous theorem.

2.3 Fixed Points and Stability

2.3.1 Determining the fixed points (Period-1)

Recall the quadratic map $f_c(z) = z^2 + c$, $c \in \mathbb{C}$. A fixed point $z^* \in \mathbb{C}$ is a point that satisfies the following equation:

$$z^* = f(z^*) = (z^*)^2 + c. \implies (z^*)^2 - z^* + c = 0$$

This is a quadratic equation in z^* . The solutions are given by the quadratic formula:

$$z^* = \frac{1 \pm \sqrt{1 - 4c}}{2}$$

This determines the fixed points under one iteration of the quadratic map, we say that these are periodic points of period-1.

2.3.2 Stability of fixed points (Period-1)

The stability of a fixed point is determined by the *derivative* of the map $f_c(z)$ evaluated at the fixed point. The derivative of the quadratic map is:

$$f'_c(z) = 2z$$

At a fixed point z^* , the stability is determined by the absolute value of $f'_c(z^*)$:

- **Attracting Fixed Point:** If $|f'_c(z^*)| < 1$, the fixed point is stable, and nearby points will converge to z^* under iteration.
- **Repelling Fixed Point:** If $|f'_c(z^*)| > 1$, the fixed point is unstable, and nearby points will diverge from z^* .
- **Indifferent Fixed Point:** If $|f'_c(z^*)| = 1$, the fixed point is neither attracting nor repelling, and the dynamics near z^* can be periodic or chaotic, depending on the higher-order behaviour of the system.

2.4 Mandelbrot Set and Julia Sets

The following definition and theorem are adapted from 2.1 in [4].

Definition (Mandelbrot set). *The **Mandelbrot set** is the set $M = \{c \in \mathbb{C} \mid \exists s \in \mathbb{R}, \forall n \in \mathbb{N}, |f_c^n(0)| \leq s\}$, where $f_c^n(z)$ is the n th iteration of $f_c(z)$. So unlike the filled Julia set, the Mandelbrot set M is the set of all c values such that the sequence $0, f_c(0), f_c(f_c(0)), \dots$ does not escape to infinity.*

Theorem 3. *For $c \in \mathbb{C}$, the point c is in the Mandelbrot set M if and only if its corresponding filled Julia set J_c is connected.*

¹Source code is found at the end of this article

From the definitions of both types of sets, the Mandelbrot set and Julia sets both arise from the quadratic map $f_c(z) = z^2 + c$. The Mandelbrot set M consists of complex parameters c where the critical point $z = 0$ remains bounded under iteration. Julia sets J_c , defined for a fixed c , form the boundary between points that escape to infinity and those that remain bounded. Their structure depends on c : if $c \in M$, the Julia set is connected; otherwise, it is a disconnected fractal.

3 NUMERICAL SIMULATION AND VISUALIZATION

3.1 Numerical Methods

Here is an algorithm¹ for generating a regular Julia set:

1. Create a grid for complex numbers using `numpy.meshgrid`.
2. Iterate the function $z_{n+1} = z_n^2 + c$ for all initial values z_0 in the complex number grid.
3. `matplotlib` library is used to visualize the coloured fractal image.
4. Calculate the fixed points and analyze their stability, then plot them into the fractal image.

Here is an algorithm for generating a zoomed-in Julia set:

Remark. To show the self-similarity of Julia sets, another program for computing a specific zoomed-in region is written.

1. Create a grid with a larger mesh.
2. Set the maximum and minimum of x and y coordinates for the desired zoomed-in region.
3. Iterate the same function but with a higher maximum iteration for better resolution.

These algorithms assign colours automatically based on the number of iterations required for the starting point to diverge to infinity. No specific values are set to determine if the point diverges, since the algorithms use `inferno` to assign colours which create a detailed fractal image. For improved clarity, higher grid resolution and zooming techniques reveal the complex self-similar structure of the Julia set. Efficient computation and visualization are achieved through vectorized numerical operations and colour mapping.

3.2 Results

Example plots (period-1 fixed points are shown in Figure 1 and Figure 3-6 just for reference):

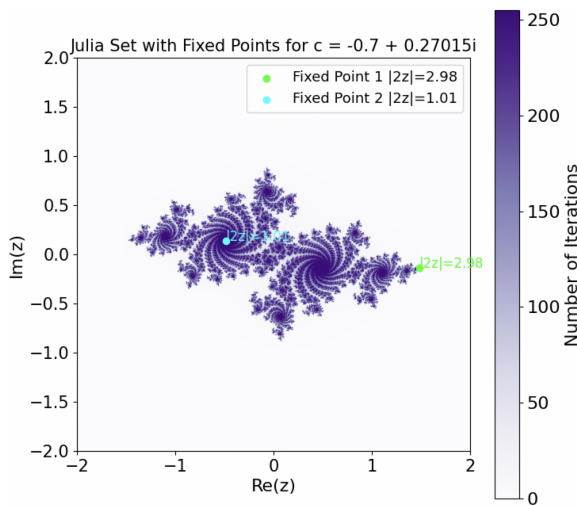


Figure 1: Julia set for $c = -0.7 + 0.27015i$.

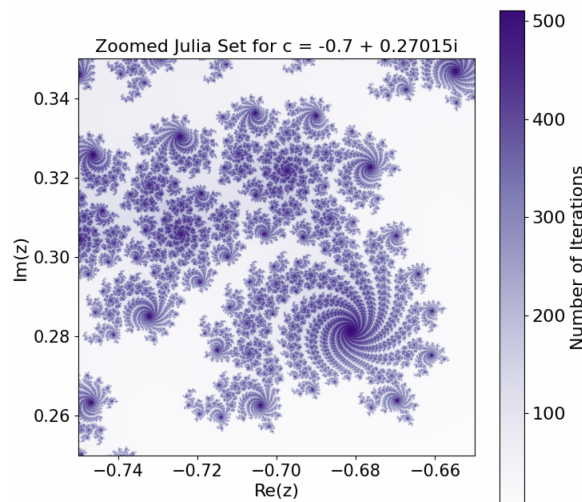


Figure 2: Zoomed-in region of the Julia set showing self-similar structure.

4 JULIA SET CLASSIFICATIONS

4.1 Connected vs. Disconnected

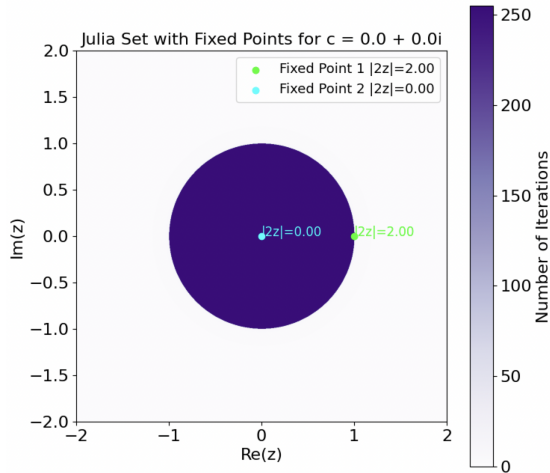
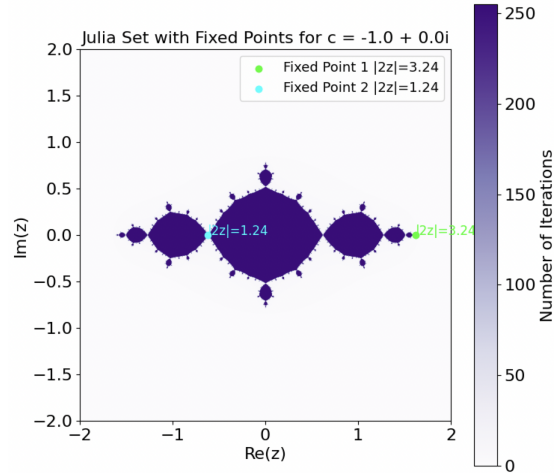
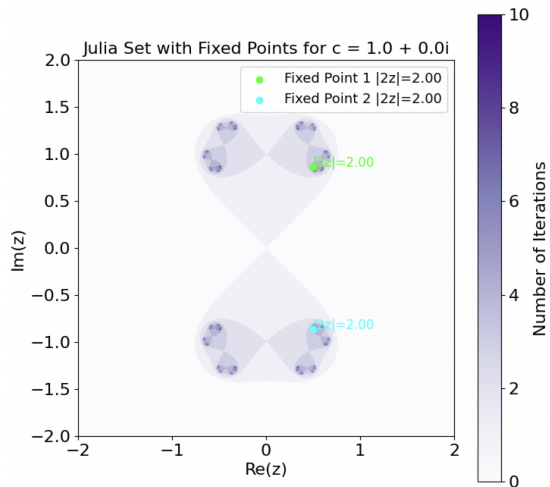
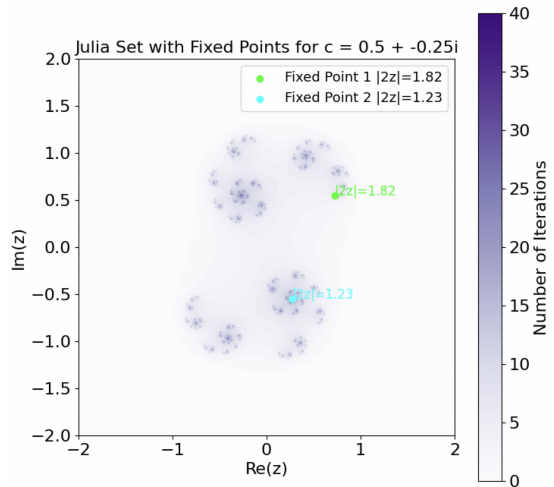
According to the **Dichotomy Theorem**, a Julia set is either connected or totally disconnected. We will vi-

sually show the difference between them with selected values of c .

Selecting $c \in M$ where M is the Mandelbrot set ensures that the Julia set J_c generated by such c is connected. Figure 3 is the Julia set generated by $c_1 = 0$; clearly c_1 is in the Mandelbrot set since $f_0(z)$ remains 0 under iteration. We can see that this non-fractal pattern is a unit circle with $(0,0)$ as the center. By colour distribution, all the points outside the unit circle diverge to infinity, while the points inside the unit circle stay bounded as the iteration goes on.

For Figure 4 with $c_2 = -1$, applying the iteration of $z \mapsto z^2 + c_2$ produces the sequence $0, -1, 0, -1, \dots$, which is bounded. Therefore, $c_2 \in M$, and the corresponding Julia set is connected. However, its structure is quite different from that of $c_1 = 0$. This filled Julia set exhibits perfect symmetry about the real axis and imaginary axis, due to the map $f_{-1} = z^2 - 1$ preserving symmetry in both the real and imaginary components of z . The main body is centred at $z = 0$, and intricate branches radiate outward forming a connected, dendritic structure. No “dust” or disconnected components are visible, indicating that the entire set is one continuous object in the complex plane. Scott Sutherland describes this structure as the “Basilica” [10], a name inspired by its resemblance to basilica architecture.

For Figure 5 with $c_3 = 1$, the sequence generated by taking iterations is $0, 1, 2, 5, 26, \dots$, which tends to infinity. Therefore, $c_3 \notin M$, and the Julia set generated by such a c_3 is not connected. The same applies to Figure 6 with $c_4 = 0.5 - 0.25i$, which is also disconnected. We find some similarities by comparing Figure 6 with Figure 5. Both images show a lighter appearance. This is because most of the points in the complex plane under the iterations generated by f_{c_3} and f_{c_4} diverge to infinity so fast that most of the points do not “survive” after 40 iterations. On the other hand, by definition, the points in connected filled Julia sets remain bounded regardless of the number of iterations applied. By looking at the scale at the left of the image, in which the Python program set the maximum iterations for each point at 256, all the points inside the unit circle, or the “Basilica” structure, have a dark purple colour, indicating they do not escape to infinity within the iterations. If we set the maximum higher, we would still see that they stay bounded.

Figure 3: Julia set for $c = 0$ Figure 4: Julia set for $c = -1$ Figure 5: Julia set for $c = 1$ Figure 6: Julia set for $c = 0.5 - 0.25i$

Conversely, the brighter regions represent points that quickly diverge. This suggests that these points are far from the filled Julia set's boundary, that is, the Julia set, and escape rapidly to infinity. All four figures have such areas, but the lower two have most of the area of the complex plane brightened. The reason for that is that the critical point at $z = 0$ escapes to infinity quickly so that it goes almost white in both figures, which causes disconnected "islands" and "dust particles" structures, in Figure 5 and Figure 6 respectively.

4.2 The Use of Escape-time Algorithm

The visualizations generated by technical tools are helpful and allow us to understand these concepts more intuitively. By iterating the quadratic mapping and ob-

serving the resulting fractals, we can clearly distinguish between connected and disconnected Julia sets. The use of the escape-time algorithm, which visualizes the escape times using gradient colours, provides a convenient and practical way to visualize and classify Julia sets.

5 QUASI-SELF-SIMILARITY OF JULIA SETS

5.1 Mathematical Foundation

To discuss the self-similarity of Julia sets theoretically, we recall some definitions from P. de la Harpe regarding pseudo-metric spaces [3].

Definition (Pseudo-metric space). A *pseudo-metric*

space is a set X , together with a function $d : X \times X \rightarrow \mathbb{R}$, called a metric or distance function, satisfying the following properties for all $x, y, z \in X$:

1. **Non-negativity:** $d(x, x) \geq 0$.
2. **Symmetry:** $d(x, y) = d(y, x)$.
3. **Triangle inequality:** $d(x, z) \leq d(x, y) + d(y, z)$.

Note that the difference between a pseudo-metric space and a metric space is that the distance between two distinct points can be zero. If d is a pseudo-metric on X , then we say (X, d) is a pseudo-metric space equipped with metric d .

Definition (Quasi-isometry). Let X, X' be two pseudo-metric spaces. A mapping $\phi : X \rightarrow X'$ is called a quasi-isometric embedding if there exist constants $K \geq 1$ and $C \geq 0$ such that for all $x, y \in X$,

$$\frac{1}{K}d(x, y) - C \leq d'(\phi(x), \phi(y)) \leq Kd(x, y) + C$$

Furthermore, ϕ is a quasi-isometry if there exists a constant $D \geq 0$ such that every point in X' is within distance D of some point in $\phi(X)$. In this case, the spaces X and X' are said to be quasi-isometric.

Now, we define the concept of quasi-isometry in the context of Julia sets. The following theorem was first established by Sullivan, and we state it in the formulation given by Monard [7].

Theorem 4 (Sullivan Theorem). Recall the map $f_c : z \mapsto z^2 + c$, for $c \in \mathbb{C}$. The Julia set J_c of f_c is such that there exists $K \geq 1$ and $r_0 > 0$ such that for every $z \in J_c$ and every $0 < r < r_0$, the set $J_c \cap D_r(z)$, where $D_r(z) = \{x \in J_c \mid d(z, x) < r\}$, dilated by a factor $\frac{1}{r}$, is K -quasi-isometric to the whole of J_c .

This theorem essentially states that if we zoom in on a small portion of the Julia set, the structure should resemble the whole set.

5.2 Qualitative Difference Between Quasi-self-similarity and Exact Self-similarity

Below are two examples of exactly self-similar fractals. They are built using a repetitive process where smaller pieces mimic the shape of the larger structure in the exact same structure but on a smaller scale.

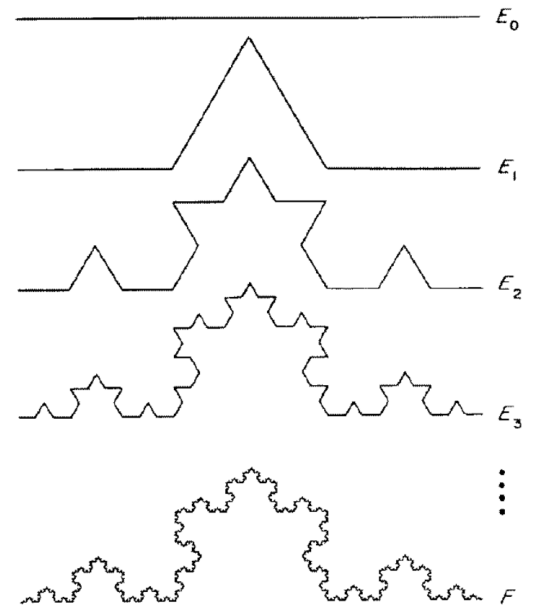


Figure 7: Construction of the von Koch curve [11]

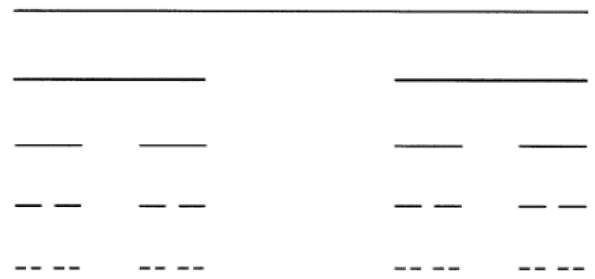


Figure 8: Cantor Set [2]

For example, to generate a von Koch curve, start with straight line segments (or equilateral triangles for a Koch snowflake). Divide each line segment into three equal parts, then replace the middle segment with two line segments, forming an equilateral triangle pointing outward. This creates a “bump” on the line. Repeat this process for each line segment. With each iteration, the curve becomes more detailed, adding more “bumps” while maintaining its fractal structure and its exact self-similarity. As iterations continue indefinitely, the length of the curve becomes infinite, but it remains confined to a finite area.

Why are Julia sets not exactly self-similar? We will discuss this by zooming in on a specific Julia set.

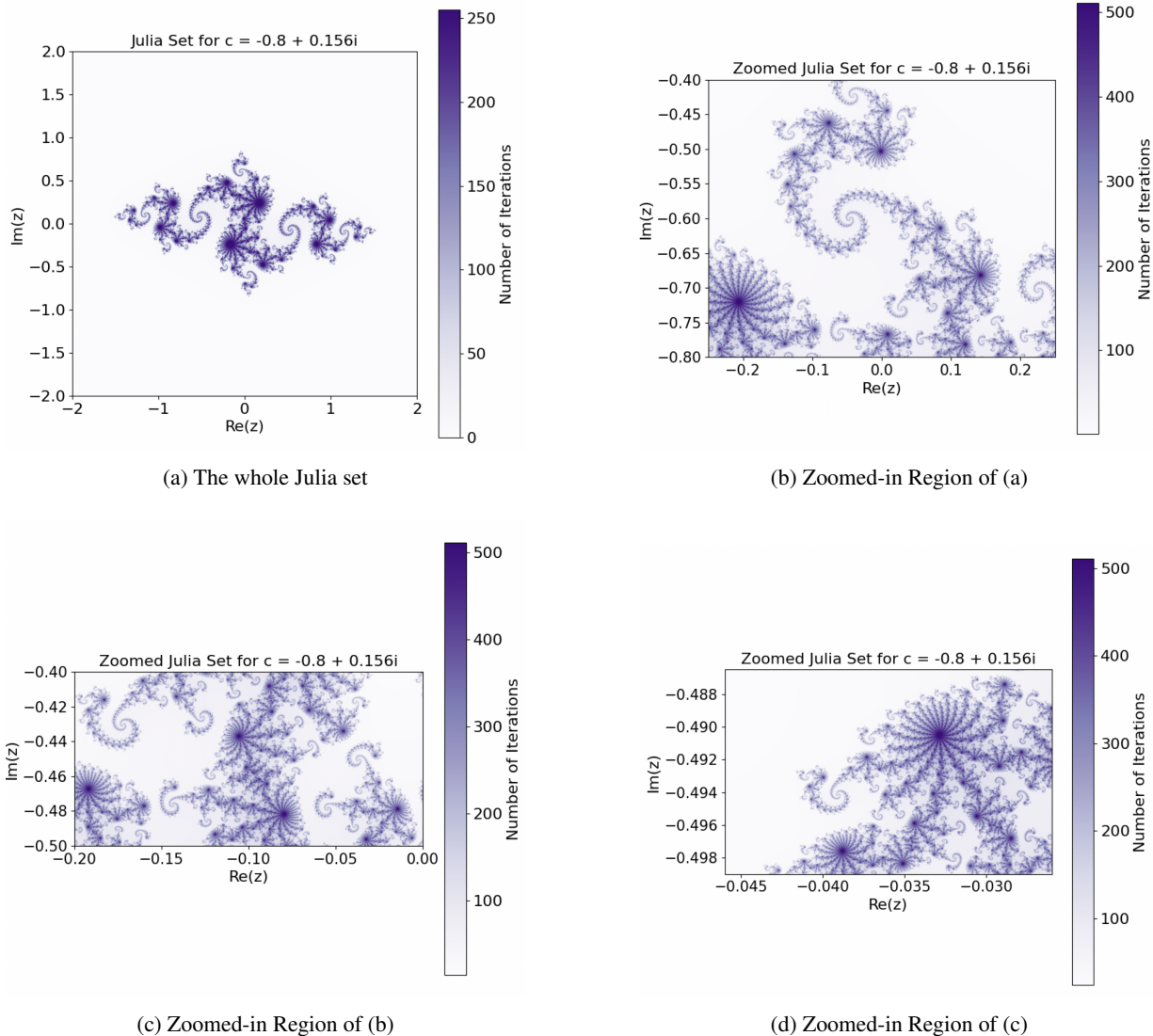


Figure 9: Julia set for $c = -0.8 + 0.156i$

Image (a) of Figure 9 is a full image of the Julia set generated by $c = -0.8 + 0.156i$: the whole image presents a “Chinese Dragon”-like structure, with two big “spirals” on both positive and negative real-axis.

Image (b) zooms in on a smaller region of the original Julia set, focusing on a segment of the boundary. Zooming in reveals a smaller spiral and complex branching patterns that resemble the structure seen in the global view: notice that if we rotate this image counter-clockwise by 45 degrees then we get a similar structure as the left side of image (a). The colour bar, indicating the iteration count, shifts to accommodate the increased resolution, emphasizing the computational intensity of capturing the details.

As we keep zooming in, the more elaborate pattern is revealed in images (c) and (d). The structure is pre-

served, and new layers of spiral-like complex substructures become visible. We can see multiple small copies around the “main body” of the structure, while the “main body” itself remains part of a larger spiral on a broader scale.

Julia sets are classified as quasi-self-similar fractals, rather than exactly self-similar fractals, because while they exhibit repeating patterns at different scales, these repeats are not identical, but rather distorted, altered, or modified in subtle ways that we may not be able to see with human vision easily. This means that arbitrarily small portions of the set can be magnified and then smoothly distorted to resemble a larger part of the set [5].

The behaviour of points on the complex plane is highly sensitive to initial conditions. Even small changes in

position can result in drastically different divergences. This sensitivity arises from the nature of the iterative process and the complex dynamics involved. While this sensitivity leads to the complex structure of the Julia set, it is not the main reason for its quasi-self-similarity, which arises from the mathematical properties of the iterative function itself, resulting in similar but not identical patterns at different scales.

6 FIXED/PERIODIC POINTS OF DIFFERENT PERIODS

6.1 Periodic Points and their stability of Period- n

We defined the periodic points and the stability of the period-1 fixed points. In this section, we will extend these definitions to higher periods.

Definition (Periodic point). A point z_0 in the complex plane is called a periodic point of period p for the function $f_c(z) = z^2 + c$ if it satisfies the following condition:

$$f_c^p(z_0) = z_0$$

where f_c^p denotes the p -th iterate of f_c , i.e.,

$$f_c^p(z) = \underbrace{f_c(f_c(\dots f_c(z)\dots))}_{p \text{ times}}$$

In other words, a point z_0 is periodic if, after p iterations of the function, it maps back to itself. The smallest such p is called the period of the point.

By computing the roots of the polynomial $F_p(z, f) = f_c^p(z) - z$ of degree 2^p , we will find the periodic points for the specific p .

Remark. Notice that the polynomial of degree 2^p has exactly 2^p complex solutions (periodic points) counted with multiplicity.

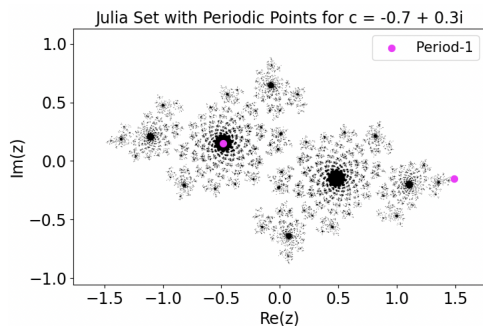


Figure 10: Julia set with periodic points of $p = 1$

6.1.1 Stability of Periodic Points

Milnor gives a precise definition of the stability of periodic points [1], which I will now adopt.

Consider a *periodic orbit* or “cycle”:

$$f : z_0 \mapsto z_1 \mapsto \dots \mapsto z_{p-1} \mapsto z_p = z_0$$

If the points z_1, \dots, z_p are all distinct, then the product of derivatives

$$\lambda = (f^p)'(z_i) = f'(z_1) \cdot f'(z_2) \cdot \dots \cdot f'(z_p) \quad (4)$$

is a well-defined complex number called the *multiplier* or the *eigenvalue* of this periodic orbit.

Similarly to the case of period-1 stability, we will classify the stability of periodic points in higher periods with the multiplier.

A periodic point is:

- **Attracting** when $|\lambda| < 1$:
 - **Super-attracting** when $\lambda = 0$;
 - **Attracting but not super-attracting** when $0 < |\lambda| < 1$;
- **Indifferent** when $|\lambda| = 1$:
 - **Rationally indifferent** if λ is a root of unity;
 - **Irrationally indifferent** if $|\lambda| = 1$ but the multiplier is not a root of unity;
- **Repelling** when $|\lambda| > 1$.

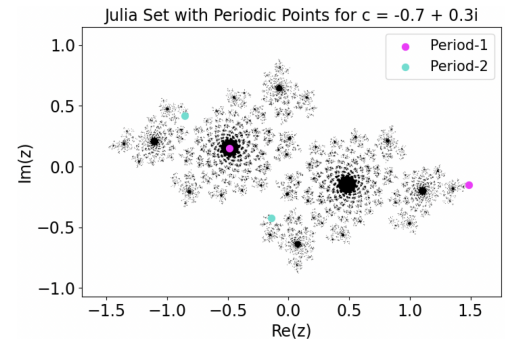


Figure 11: Julia set with periodic points of $p = 1, 2$

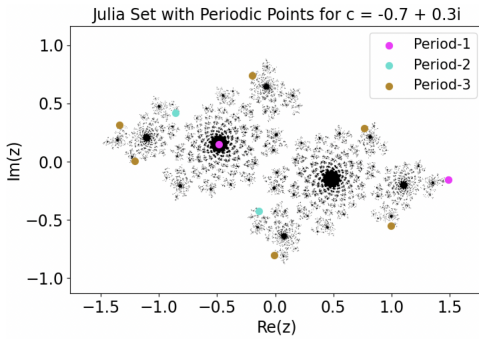


Figure 12: Julia set with periodic points of $p = 1, 2, 3$

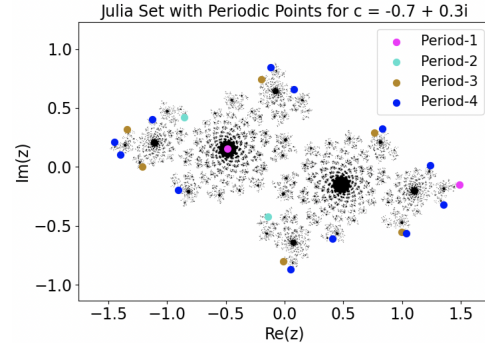


Figure 13: Julia set with periodic points of $p = 1, 2, 3, 4$

6.2 Example of Julia Set With Their Periodic Points of Different Periods

We now compute and visualize the periodic points of the Julia set generated by $c = -0.7 + 0.3i$ by iterating the quadratic map and finding the roots of the final composite polynomial. To emphasize those points, we keep other points in the Julia set black.

Figures 10-13 show an increase in periodic points as periods increase. In period 1, there are only $2^1 = 2$ periodic (or fixed) points, and in period 2, there are $2^2 = 4$ periodic points, and so on. For each periodic point, the algorithm colours points with the colour corresponding to their *minimal* period. Notice that there are a total of 4 periodic points in period 2, but only two of them are in the turquoise colour, the other two remain fuchsia. That is because, by the property of periodic points, period 1 fixed points have a periodic orbit of period 1, i.e. $f : z_0 \mapsto z_0$, under every iteration, thus they remain the same forever and are always the roots of F_p function for all period p . Similarly, periodic points of $p = 2$ will return to their original points under 2 iterations. So periodic points of $p = 2$ are also periodic points of $p = 4$, essentially completing two full periodic orbits of $f : z_0 \mapsto z_1 \mapsto z_2 = z_0$. This demonstrates the basic property of periodic points and gives a good intuition on understanding their behaviour in the dynamical plane.

6.2.1 Stability of Periodic Points

We can easily compute the multiplier using equation (4) from section 6.1.1 numerically. It turns out all the periodic points from period 1 to period 6 in the example are repelling, that is, no finite attractor was

found. This is expected, as the chosen c lies near the boundary of the Mandelbrot set. We will now discuss how the choice of c may impact the stability of periodic points. This idea is adapted from a project by 3D-XplorMath [9], a freely available mathematical visualization program that presents various mathematical objects and processes. This program is monitored by the 3DXM Consortium, an international volunteer group of mathematicians.

Experimental Findings: If c is in the *interior* of Mandelbrot set M (*interior*: some neighbourhood of c is also in M), then iterating the map $f : z \mapsto z^2 + c$ results in exactly one attracting periodic orbit.

1. If c is in the main cardioid (large, heart-shaped region) of M , f_c has an attracting fixed (or period 1) point.
2. If c is in the open circular chest of M , then such an iterating map has an attracting periodic orbit of period 2.
3. If c is in the two biggest disks attached to the main cardioid, then such an iterating map has an attracting periodic orbit of period 3.
4. If c is a boundary point of M , then such an iterating map may not have any attracting periodic orbit other than infinity.

A good example is J_c with $c = 0$ as shown in Figure 3. Obviously, such c is inside the main cardioid of the Mandelbrot set, and it has a super-attracting fixed point at $z = 0$. Every point outside the unit circle is moving to infinity.

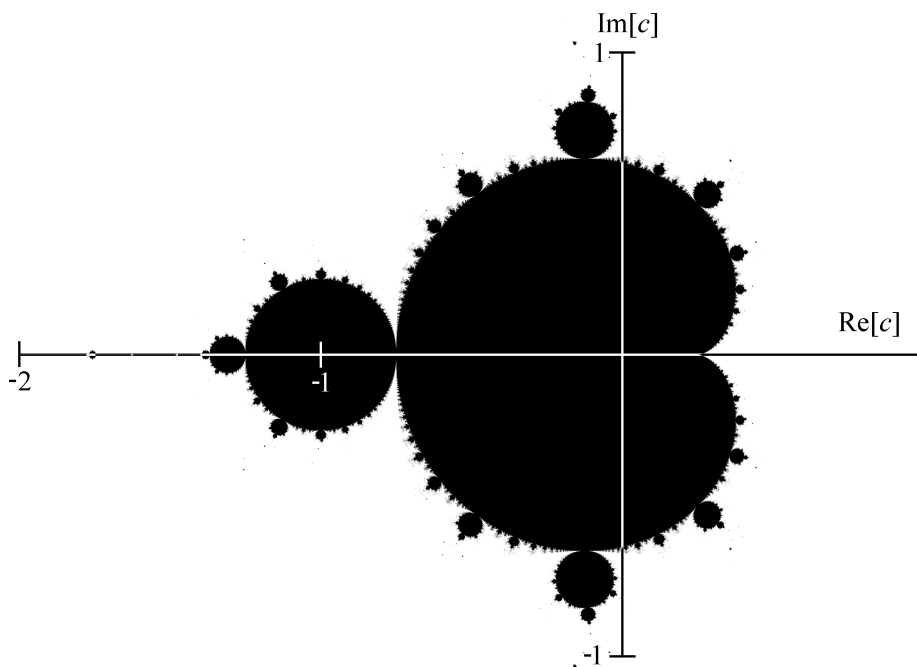


Figure 14: Mandelbrot Set [12]

7 CONCLUSION

This project explored the dynamics of Julia sets. By studying the iterative behaviour of quadratic mappings, we classified Julia sets into connected and disconnected types, emphasizing their dependence on the value of c and its position relative to the Mandelbrot set.

Through numerical simulations and visualizations, we demonstrated the complex structure of Julia sets and their quasi-self-similar fractal properties. These visualizations showed how mathematical theories can be transformed into compelling graphical representations.

This project offered an opportunity to study the interaction between theory and computation, giving a glimpse into the mysterious world of fractals. Hopefully, it will inspire further curiosity for future explorations.

REFERENCES

- [1] John Milnor. *Dynamics in One Complex Variable: Introductory Lectures (Partially revised version of 9-5-91)*. Accessed: 2025-02-12. 1991.
- [2] Catherine Bovill. *The Self-Similarity Pattern of Cantor Set*. Online Image. Accessed: 2025-02-12. 1996. URL: https://www.researchgate.net/figure/The-self-similarity-pattern-of-cantor-set-Source-Bovill-1996_fig1_376644126.
- [3] P. de la Harpe. *Topics in Geometric Group Theory*. Chicago Lectures in Mathematics. University of Chicago Press, 2000. ISBN: 0-226-31719-6.
- [4] Stephanie Avalos-Bock. *Fractal Geometry: The Mandelbrot and Julia Sets*. July 2009. URL: <http://www.math.uchicago.edu/~may/VIGRE/VIGRE2009/REUPapers/Avalos-Bock.pdf>.
- [5] Kenneth Falconer. *Fractal Geometry: Mathematical Foundations and Applications, 3rd Edition*. Wiley, 2014, p. 400. ISBN: 978-1-119-94239-9.
- [6] Michael Frame and Amelia Urry. *Fractal Worlds: Grown, Built, and Imagined*. Yale University Press, 2015. ISBN: 978-0-300-19787-7.
- [7] Francois Monard. *Lecture 20: Introduction to complex dynamics - 3/3: Mandelbrot and friends*. Accessed: 2025-02-12. 2017. URL: https://people.ucsc.edu/~fmonard/Sp17_Math207/lecture20.pdf.
- [8] IBM. *Benoit B. Mandelbrot: The Father of Fractals*. Accessed: 2025-02-12. 2025. URL: <https://www.ibm.com/history/benoit-mandelbrot>.
- [9] Virtual Math Museum. *Julia Sets*. Accessed: 2025-02-12. 2025. URL: <https://virtualmathmuseum.org/Fractal/julia/index.html>.
- [10] Scott Sutherland. *AN INTRODUCTION TO JULIA AND FATOU SETS*. Accessed: 2025-02-12.

url: <https://www.math.stonybrook.edu/~scott/Papers/India/Fatou-Julia.pdf>.

- [11] Unknown Author. *Construction of the von Koch Curve*. Online Image. Accessed: 2025-02-12. Accessed 2025. URL: https://www.researchgate.net/figure/Construction-of-the-von-Koch-curve-F-At-each-stage-the-middle-third-of-each-interval_fig5_26365833.

- [12] Ruben van Nieuwpoort. *Mandelbrot Set Visualization*. Online Image. Accessed: 2025-02-12. Accessed 2025. url: https://paulbourke.net/fractals/mandelbrot/Ruben_van_Nieuwpoort.html.

CODE LISTINGS

<https://github.com/gabriellachenmq/JuliaSetsCode>

	2			3		9		7
	1							
4		7				2		8
		5	2				9	
			1	8		7		
	4				3			
				6			7	1
	7							
9		3		2		6		5

Fun fact: The minimum amount of clues for a sudoku puzzle to be solvable is 17!

is concerned with the *justification* of mathematics. Never mind *how* mathematicians got to real analysis, or group theory: what matters to the formalist is that we can prove the results of these domains. *Proofs and Refutations*, meanwhile, is centrally concerned with how mathematics develops in the first place. In particular, Lakatos argues that mathematics does not emerge from deductions and axioms alone, as the formalists suggest. Rather, mathematics advances thanks to trial and error, proof-attempts, and counterexamples.

Lakatos' diatribe against formalism mostly takes the form of a dialogue between students in a classroom (named Greek letters) and a teacher. In this setting, Lakatos recreates the history of the development of a proof for Euler's conjecture: that for all polyhedra, the number of vertices (V), edges (E), and faces (F) satisfies the relation $V - E + F = 2$. At this point, I encourage the reader to pause and consider some of their favourite polyhedra and check if the conjecture holds.

In most cases, one will find the conjecture to hold, unless they have picked a particularly exotic polyhedron. But the question then emerges: how would one go about *proving* the statement $V - E + F = 2$ for all polyhedra? It is at this point that the students in Lakatos' classroom begin their discussion. Meanwhile, in the footnotes, Lakatos reconstructs the historical development of a proof for Euler's conjecture.

What becomes clear through the text is the fact that this process is anything but logical and deductive. While the students begin with a "proof-idea" inspired by Augustin-Louis Cauchy, a string of refutations quickly run up against this proof-attempt. In response, the teacher chimes in to suggest that proofs do not need to "prove" what they set out to prove [2, p. 14]. We will soon see what he means.

The class' many counterexamples lead to a discussion of how a proof's refutations should be handled. One camp, called *monster-barrers* rejects these refutations: they take them as "monsters" that should not be considered, because they violate the perfection of the proof [2, p. 14]. From this, we get the question of what a polyhedron actually *is*—that is, what kinds of objects are valid for consideration for this conjecture? An alternative camp, the *exception-barrers*, use refutations to define the domain of validity for their conjecture [2, p. 34]. By carefully analyzing the proof and its constitutive lemmas, the best exception-barrers identify the conditions that allow a counterexample to arise in the first place. Then, they incorporate these conditions into the conjecture itself, therein protecting it from the counterexample.

This strategy, called *lemma-incorporation*, preserves the original lemmas while refining the conjecture to clarify its explanatory scope [2, p. 36]. Using this method, the specific conditions that bar a given counterexample are integrated into the conditions of the conjecture. Through this process, Cauchy's proof-idea of the statement, "for all polyhedra $V - E + F = 2$ " turns into "for a simple polyhedron, whose faces are all simply connected, $V - E + F = 2$."¹

Using lemma-incorporation, counterexamples are not monsters to be avoided, but tools for refining a conjecture. We can understand the original statement "for all polyhedra $V - E + F = 2$ " as a "primitive" conjecture, which the class then refined using lemma-incorporation. This explains the teacher's willingness to entertain proofs of conjectures that may turn out to be false, as they help refine the conjecture and make explicit the conditions under which it holds.

Through the dialogue, Lakatos explains how lemma-incorporation exemplifies the intrinsic link between proofs and refutations. By subjecting conjectures to criticism, mathematicians can refine their initial ideas, making explicit the previously hidden conditions under which they hold. For Lakatos, this interplay between a proof and refutations illustrates how justification and discovery in mathematics are unified. Proofs that fail to "prove" often pave the way for better-formulated theorems.

However, the teacher emphasizes that this method is rarely used, since most people expect their theories to advance monotonously toward truth. Lakatos argues, however, that counterexamples should be seen as opportunities to refine conjectures. This is why the best exception-barrers begin by proving their conjecture within a "safe" domain, then subject it to critical investigation. This process may lead to provisional theorems barring certain counterexamples, which are further refined through lemma-incorporation. Unlike monster-barring, this approach does not suppress criticism. Rather, it pushes refutations to the background, allowing a conjecture to expand outward from a secure foundation [2, p. 36–37].

Lakatos christens this method of simultaneous discovery and justification *the method of proof and refutations*. Revealing the unity of a proof and refutations, the method improves proofs by integrating proof-attempts into the statement and eventual proof of the conjecture [2, p. 37]. However, Lakatos, through student Alpha, remarks that this process is indiscernible in the end-product of mathematical discovery. In general, one cannot see the back-and-forth process of the

¹As a historical note, it is by discussing polyhedra with the goal of proving Euler's conjecture that concepts like "simple polyhedra" and "simply connectedness" became articulated by Cauchy and others in the first place. Indeed, Lakatos attributes the development of the field of algebraic topology to the attempt to prove for all polyhedra, $V - E + F = 2$. For more on this discussion, I urge the reader to see [3]. This view of the historical development of algebraic topology is characteristically Lakatosian, and contributes to his view of the utility of counterexample in the development of mathematics.

COMPUTATIONAL ASPECTS OF MODULAR FORMS

Ben Merbaum

This work is derived from my MATH 470 Honours Undergraduate Research Project. My project introduces the theory of modular forms and Hecke operators. The space of cusp forms, a subset of modular forms, can be endowed with an inner product structure under which one can find an orthonormal basis of eigenfunctions. In this article I provide an introduction to this theory and show how one can compute an eigenbasis for arbitrary spaces of cusp forms. While this theory is relatively new in the timeline of mathematics (within the last two centuries), the advancement of understanding of modular forms has enabled significant progress in analytic number theory and algebraic geometry.

1 INTRODUCTION

Modular forms often arise in unexpected yet exciting contexts, providing the tools to find exact solutions of quintic equations or solve Fermat's Last Theorem. A 2017 proof by Maryna Viazovska used modular forms to prove the densest arrangement of unit spheres in 8-dimensional space, known as the sphere packing program [3]. Constructions of modular forms combine theories of complex analysis, algebra, number theory, and topology, and the insights derived from modular forms often apply to many distinct areas of mathematics.

When we equip the space of modular forms with the action of Hecke operators, then we can guarantee the existence of an orthonormal basis of Hecke eigenfunctions which have certain nice behaviour. However, these eigenfunctions are often non-trivial to compute. I will first introduce the intricate structure of these functions, and I will then use certain algebraic relations to detail a general method for computing eigenfunctions.

These computations allow for concrete classification of modular forms, which arise first as abstract objects. For instance, when one first sees the definition of a vector space V , a natural problem arises about how to list *all* the vectors in V . This requires finding an isomorphism $V \cong \mathbb{R}^n$ and writing the vector elements of V as n -tuples. In the same way, we can use Hecke eigenfunctions and the computations shown here to naturally describe how to list *all* the modular forms of a given weight.

2 MODULAR FORMS

Let $\mathcal{H} = \{z \in \mathbb{C} : \text{Im}(z) > 0\}$ be the upper half-plane of the complex numbers. Let $\Gamma(1) := \text{PSL}_2(\mathbb{Z}) = \text{SL}_2(\mathbb{Z})/\{\pm 1\}$ be the *modular group*, which acts faithfully on \mathcal{H} by Möbius transformations: $\begin{pmatrix} a & b \\ c & d \end{pmatrix} z = \frac{az+b}{cz+d}$.

Definition. Let $f : \mathcal{H} \rightarrow \mathbb{C}$ be holomorphic, then we say f is a modular form of weight $2k$ ($k \in \mathbb{N}$) if:

$$(i) f\left(\frac{az+b}{cz+d}\right) = (cz+d)^{2k} f(z) \text{ for all } \begin{pmatrix} a & b \\ c & d \end{pmatrix} \in \Gamma(1).$$

(ii) f has a Fourier expansion at ∞ given by

$$f(z) = \sum_{n=0}^{\infty} a_n q^n \text{ where } q = e^{2\pi iz}, a_n \in \mathbb{C}$$

which converges in $\{z \in \mathcal{H} : \text{Im}(z) > T\}$ for some $T > 0$ (which we refer to as converging as $z \rightarrow \infty$).

If $f(\infty) = a_0 = 0$, we say f is a cusp form of weight $2k$. We define the following vector spaces:

$$M_{2k} = \{\text{modular forms of weight } 2k\},$$

$$M_{2k}^0 = \{\text{cusp forms of weight } 2k\}.$$

Remark. For a more natural derivation of the definition of modular forms, see [1] or [2].

Example. For $k \geq 2$, the Eisenstein series of weight $2k$ is given by

$$E_{2k}(z) = \frac{1}{2 \cdot \zeta(2k)} \sum_{\substack{m,n \in \mathbb{Z} \\ (m,n) \neq (0,0)}} \frac{1}{(mz+n)^{2k}}$$

where ζ is the Riemann zeta function. This satisfies $E_{2k}(\text{inf}) = 1$ and has Fourier expansion given by

$$E_{2k}(z) = 1 + \frac{(2\pi i)^{2k}}{(2k-1)! \zeta(2k)} \sum_{n=1}^{\infty} \sigma_{2k-1}(n) q^n$$

where $\sigma_k(n) := \sum_{d|n} d^k$.

Example. The modular discriminant Δ is a cusp form of weight 12 given by

$$\Delta(z) = (120\zeta(4)E_4(z))^3 - 27(280\zeta(6)E_6(z))^2$$

An identity by Jacobi gives

$$\Delta(z) = (2\pi)^{12} q \prod_{n=1}^{\infty} (1 - q^n)^{24} = (2\pi)^{12} \sum_{n=1}^{\infty} \tau(n) q^n$$

Hence, $\Delta(\infty) = 0$ and $\tau(1) = 1$. We call $\tau : \mathbb{N} \rightarrow \mathbb{Z}$ the Ramanujan τ function. We will see that τ is a multiplicative function.

Theorem 1.

- (i) $M_{2k} \cong M_{2k}^0 + \mathbb{C}E_{2k}$ and $\dim M_{2k} = \dim M_{2k}^0 + 1$.
- (ii) $f \mapsto \Delta \cdot f$ induces an isomorphism $M_{2k-12} \cong M_{2k}^0$.
- (iii) $\dim M_{2k} = \begin{cases} 0 & \text{if } k < 0 \\ \lfloor k/6 \rfloor & \text{if } k \geq 0, k \equiv 1 \pmod{6} \\ \lfloor k/6 + 1 \rfloor & \text{if } k \geq 0, k \not\equiv 1 \pmod{6}. \end{cases}$

Proof. [2, Theorem 3.10] □

Example. The spaces M_4, M_6, M_{12}^0 are of dimension 1 and generated by $E_4, E_6,$ and $\Delta,$ respectively.

3 THE HECKE OPERATORS

Definition. Let $n \geq 1, f \in M_{2k},$ then the n^{th} Hecke operator applied to $f,$ denoted $T(n)f,$ is given by

$$T(n)f(z) = n^{2k-1} \sum_{\substack{ad=n \\ a \geq 1, 0 \leq b < d}} d^{-2k} f\left(\frac{az+b}{d}\right).$$

Remark. For a more natural derivation of Hecke operators from the theory of lattices, see [1] or [2].

Proposition 2. M_{2k} and M_{2k}^0 are stable under $T(n).$ Moreover, the following identities hold for $f \in M_{2k}$:

- (i) $T(m)T(n)f = T(mn)f$ if $\gcd(m, n) = 1,$
- (ii) $T(p)T(p^n)f = T(p^{n+1})f + p^{2k-1}T(p^{n-1})f$ if p is prime.

In particular, by applying induction on $n,$ one sees that $T(p^n)$ can be expressed as a polynomial in $T(p).$ Thus, the algebra generated by $\{T(n) : n \in \mathbb{N}\}$ is equivalent to the algebra generated by $\{T(p) : p \text{ prime}\}$ and is commutative.

Proof. [2, Proposition 10.6] □

Definition. A modular form f is an eigenform if for each $n \geq 1$ there exists $\lambda(n) \in \mathbb{C}$ such that

$$T(n)f = \lambda(n)f$$

Example. If $\dim M_{2k} = 1$ (resp. $\dim M_{2k}^0 = 1$), then any $f \in M_{2k}$ (resp. $f \in M_{2k}^0$) is an eigenform since these spaces are stable under the Hecke operator. For instance, $E_4, E_6,$ and Δ are eigenforms.

Theorem 3. Let $f(z) = \sum_{n=0}^{\infty} c(n)q^n$ be an eigenform of weight $2k > 0$ then

$$c(1) \neq 0 \text{ and } c(n) = \lambda(n)c(1) \text{ for all } n > 1.$$

Specifically, we say that f is a normalized eigenform if $c(1) = 1,$ in which case $c(n) = \lambda(n).$

Proof. [2, Theorem 10.5] □

Corollary 4. Let $f(z) = \sum_{n=0}^{\infty} c(n)q^n$ be a normalized eigenform. Then, since the numbers $\lambda(n) = c(n)$ satisfy the same relations as $T(n),$ we have:

- (1) $c(m)c(n) = c(mn)$ if $\gcd(m, n) = 1,$
- (2) $c(p)c(p^n) = c(p^{n+1}) + p^{2k-1}c(p^{n-1})$ if p is prime.

Example. In particular, letting $\Delta(z) = (2\pi)^{12} \sum_{n=1}^{\infty} \tau(n)q^n,$ then $(2\pi)^{-12}\Delta$ is a normalized eigenform and the τ coefficients satisfy the identities above. This result is commonly known as Ramanujan conjectures, posed by Srinivasa Ramanujan in 1916. While it was proven by Mordell in 1917, much of the mathematical understanding remained a mystery until the use of Hecke operators allowed Erich Hecke to prove a stronger version of this result in 1937. [2, page 61]

Definition. Let $f, g \in M_{2k}^0.$ We define the Petersson inner product on M_{2k}^0 by

$$\langle f, g \rangle = \int_D f(z)\overline{g(z)}y^{2k-2}dx dy \text{ where } z = x + iy$$

and $D = \{z \in \mathcal{H} : |Re(z)| < \frac{1}{2}, |z| > 1\}$

D is called a fundamental domain for the action of $PSL_2(\mathbb{Z})$ on \mathcal{H} by Möbius transformations.

Theorem 5. $T(n)$ is a self-adjoint operator with respect to the Petersson inner product, i.e.

$$\langle T(n)f, g \rangle = \langle f, T(n)g \rangle$$

for all $n \geq 1, f, g \in M_{2k}^0$

Proof. [1, Section 5.6] □

Using the above theorem, one can invoke the spectral theorem, which guarantees the existence of an orthonormal basis of M_{2k}^0 given by eigenfunctions of any given $T(n)$ with real eigenvalues. Since Hecke operators commute with one another, this extends to an orthonormal basis of M_{2k}^0 given by simultaneous eigenforms. Further, by 3, it follows that each λ -eigenspace is 1-dimensional. Summarizing, we have that

$$\{f \in M_{2k}^0 : f \text{ is a normalized eigenform}\}$$

is an orthonormal basis of M_{2k}^0 with respect to the Petersson inner product.

4 COMPUTING EIGENFORMS

4.1 Cusp Forms of Weight 24

We now delve into computational aspects of modular forms by showing how to compute an eigenbasis using the above identities. Since spaces with dimension 1 have trivial eigenbases (given by any function in the space), we show an example for the first space of cusp forms with dimension greater than 1, which is M_{24}^0 .

- We begin with a basis of M_{24}^0 given by $\{(2\pi)^{-12}\Delta E_4^3, (2\pi)^{-24}\Delta^2\}$. Since $\{E_4^3, (2\pi)^{-12}\Delta\}$ is a basis of M_{12} , then multiplying by $(2\pi)^{-12}\Delta$ gives rise to a basis of M_{24}^0 . Since Δ is a linear combination of E_4^3 and E_6^2 , linear independence follows from the fact that E_4^3 and E_6^2 are not scalar multiples of each other. We have the following Fourier expansions, where $q = e^{2\pi iz}$:

$$\begin{aligned} (2\pi)^{-12}\Delta(z) \cdot E_4(z)^3 &= \sum_{n=1}^{\infty} c_0(n)q^n \\ &= q + 696q^2 + 162252q^3 \\ &\quad + 12831808q^4 + O(q^5) \\ (2\pi)^{-24}\Delta(z)^2 &= \sum_{n=1}^{\infty} c_1(n) \\ &= q^2 - 48q^3 + 1080q^4 \\ &\quad - 15040q^5 + O(q^6) \end{aligned}$$

- We parameterize possible normalized eigenforms by

$$\begin{aligned} f_t &= \sum_{n=1}^{\infty} c(n)q^n \\ &= (2\pi)^{-12}\Delta(z)E_4(z)^3 + t(2\pi)^{-24}\Delta(z)^2 \text{ for } t \in \mathbb{C} \end{aligned}$$

and we must find two values $t \in \mathbb{C}$ such that f_t is an eigenform. Our coefficients satisfy

$$c(n) = c_0(n) + tc_1(n) \text{ with } c(1) = 1 + t \cdot 0 = 1$$

so our eigenforms f_t are normalized.

- We solve for t by using the following identity:

$$c(p)c(p^n) = c(p^{n+1}) + p^{2k-1}c(p^{n-1})$$

Substituting $p = 2$, $n = 1$, and $2k = 24$, we obtain:

$$\begin{aligned} c(2)^2 &= c(4) + 2^{23}c(1) \\ (696 + t)^2 &= (12831808 + 1080t) + 2^{23} \\ 0 &= t^2 + 312t - 20736000 \\ t &= -156 \pm 12\sqrt{144169} \end{aligned}$$

Therefore, our eigenbasis for M_{24}^0 is given by:

$$\left\{ \begin{aligned} &\frac{\Delta(z)}{(2\pi)^{12}}E_4(z)^3 + (-156 + 12\sqrt{144169})\frac{\Delta(z)^2}{(2\pi)^{24}}, \\ &\frac{\Delta(z)}{(2\pi)^{12}}E_4(z)^3 - (156 + 12\sqrt{144169})\frac{\Delta(z)^2}{(2\pi)^{24}} \end{aligned} \right\}$$

4.2 Cusp Forms of Weight 36

We now search for an eigenbasis for the space of cusp forms of weight 36, the first such space of dimension 3. We employ a similar procedure to the steps used for the space of weight 24, with a few modifications.

- We begin with a basis of M_{36}^0 given by $\{(2\pi)^{-12}\Delta E_4^6, (2\pi)^{-24}\Delta^2 E_4^3, (2\pi)^{-36}\Delta^3\}$.

$$\begin{aligned} (2\pi)^{-12}\Delta(z)E_4(z)^6 &= \sum_{n=1}^{\infty} c_0(n)q^n \\ &= q + 1416q^2 + 842652q^3 \\ &\quad + 271386688q^4 + 50558976510q^5 \\ &\quad + 5356057835232q^6 + O(q^7) \\ (2\pi)^{-24}\Delta(z)^2E_4(z)^3 &= \sum_{n=1}^{\infty} c_1(n)q^n \\ &= q^2 + 672q^3 + 145800q^4 \\ &\quad + 9111680q^5 - 233907300q^6 + O(q^7) \\ (2\pi)^{-36}\Delta(z)^3 &= \sum_{n=1}^{\infty} c_2(n)q^n \\ &= q^3 - 72q^4 + 2484q^5 \\ &\quad - 54528q^6 + O(q^7) \end{aligned}$$

- We parametrize possible normalized eigenforms in two variables by

$$\begin{aligned} f_{t_1, t_2} &= \sum_{n=1}^{\infty} c(n)q^n = (2\pi)^{-12}\Delta E_4^6 \\ &\quad + t_1(2\pi)^{-24} \cdot \Delta^2 E_4^3 + t_2(2\pi)^{-36}\Delta^3 \\ &\text{for } t_1, t_2 \in \mathbb{C} \end{aligned}$$

We must find three pairs $(t_1, t_2) \in \mathbb{C}^2$ such that f_{t_1, t_2} is an eigenform. Our coefficients satisfy

$$c(n) = c_0(n) + t_1c_1(n) + t_2c_2(n)$$

and

$$c(1) = 1 + t_1 \cdot 0 + t_2 \cdot 0 = 1$$

so our eigenforms f_{t_1, t_2} are normalized.

- We solve a system of two equations in terms of the Fourier coefficients of f_{t_1, t_2} to obtain t_1, t_2 :

$$\begin{aligned} \diamond c(2)^2 &= c(4) + 2^{23}c(1) \implies (1416 + t_1)^2 = \\ &\quad (271386688 + 145800t_1 - 72t_2) + 2^{23} \\ \diamond c(2)c(3) &= c(6) \implies (1416 + t_1)(842652 + \\ &\quad 672t_1 + t_2) = 5356057835232 - 233907300t_1 - \\ &\quad 54528t_2 \end{aligned}$$

Rearranging the first equation, we obtain

$$t_2 = \frac{1}{72} [-(1416 + t_1)^2 + 271386688 + 145800t_1 + 2^{23}]$$

$$= -\frac{1}{72}t_1^2 + \frac{5957}{3}t_1 + 3857920$$

Substituting into the second equation and solving the cubic equation via SageMath, we obtain the three following solutions:

- ◊ $t_1 \approx 13745.4$ and $t_2 \approx 28527662.0$.
- ◊ $t_1 \approx -114152.2$ and $t_2 \approx -403792779.0$.
- ◊ $t_1 \approx 235814.8$ and $t_2 \approx -300234403.0$.

These yield our three eigenforms f_{t_1, t_2} .

4.3 General Procedure

Using the examples in the previous two sections, we seek to formalize our procedure for computing eigenbases for the spaces of cusp forms of weight $2k$. The steps are as follows.

- Find a basis of M_{2k}^0 in terms of products of $(2\pi)^{-12}\Delta, E_4$, and E_6 :
If 12 divides $2k$, a basis is given by $\{(2\pi)^{-12}\Delta E_4^{(2k-12)/4}, (2\pi)^{-24}\Delta^2 E_4^{(2k-24)/4}, \dots, (2\pi)^{-2k/12}\Delta^{2k/12}\}$, where each term is obtained from the previous one by multiplying by $(2\pi)^{-12}\Delta$ and dividing by E_4^3 .

Otherwise, let g be a modular form of minimal weight such that the weight of g is congruent to $2k$ modulo 12 and $g(\infty) = 1$. This can be obtained as a monomial in terms of E_4 and E_6 . Then, a basis is given by $\{g(2\pi)^{-12}\Delta E_4^a, g(2\pi)^{-24}\Delta^2 E_4^{a-3}, \dots, g(2\pi)^{-b}\Delta^b\}$, where a, b are non-negative integers which ensure that the weight of each modular form sums to $2k$ and each term is obtained from the previous one by multiplying by $(2\pi)^{-12}\Delta$ and dividing by E_4^3 .

Let $\{g_0, \dots, g_r\}$ be a basis for M_{2k}^0 where $\dim M_{2k}^0 = r + 1$ and $r \geq 1$. Write

$$g_i(z) = \sum_{n=1}^{\infty} c_i(n)q^n \text{ where } q = e^{2\pi iz}$$

and suppose $c_0(1) = 1$ (g_1 has only one factor of $(2\pi)^{-12}\Delta$) and $c_i(1) = 0$ for all $i > 0$.

- Parameterize possible eigenforms in r variables by

$$f_{t_1, \dots, t_r} = g_0 + t_1 g_1 + \dots + t_r g_r \text{ with } t_1, \dots, t_r \in \mathbb{C}.$$

We must find $r + 1$ distinct r -tuples (t_1, \dots, t_r) where f_{t_1, \dots, t_r} is an eigenform. Our coefficients satisfy

$$c(n) = c_0(n) + t_1 c_1(n) + \dots + t_r c_r(n)$$

and

$$c(1) = 1 + t_1 \cdot 0 + \dots + t_r \cdot 0 = 1$$

so our eigenforms f_{t_1, \dots, t_r} are normalized.

- Solve a system of r equations in t_1, \dots, t_r by using the identities:
 - ◊ $c(m)c(n) = c(mn)$ if $\gcd(m, n) = 1$.
 - ◊ $c(p)c(p^n) = c(p^{n+1}) + p^{2k-1}c(p^{n-1})$ if p is prime.

We can choose to only solve equations of the second form. Substituting $n = 1$, we obtain:

$$c(p)^2 = c(p^2) + p^{2k-1}$$

$$(c_0(p) + t_1 c_1(p) + \dots + t_r c_r(p))^2 = c_0(p^2) + t_1 c_1(p^2) + \dots + t_r c_r(p^2) + p^{2k-1}$$

Choosing the first r primes, we can obtain r quadratic equations in r variables which can be solved via numerical analysis and computational root-finding tools. By 5, we expect to obtain exactly $r + 1$ unique solutions.

- The $r + 1$ eigenforms are given by f_{t_1, \dots, t_r} where (t_1, \dots, t_r) satisfy the above equations.

5 CONCLUSION

In this project, I described how the Hecke operators can be used to find a basis for the space of cusp forms and obtain a rich structure. Moreover, the coefficients of eigenforms satisfy nice analytic properties, and by taking the Dirichlet L-series with corresponding coefficients, we can compute an Euler product, providing connections to complex analysis and the study of prime numbers.

For future work in this area of computational number theory, it would be interesting to compare the efficiency of the above procedure with different bases and systems of equations. This can be formalized rigorously with the ideas of computational complexity theory to measure the time complexity of our procedure.

REFERENCES

[1] J.P. Serre. *A Course in Arithmetic*. Graduate texts in mathematics. Springer, 1973.

[2] J. Silverman. *Advanced Topics in the Arithmetic of Elliptic Curves*. Graduate texts in mathematics. Springer, 1994.

[3] Maryna Viazovska. The sphere packing problem in dimension 8. *Annals of Mathematics*, 185(3), May 2017.

RECIPE: GOAT CHEESE AND ASPARAGUS TART

Helena Heinonen — save this simple recipe to make for π -day!

INGREDIENTS

- 170g all-purpose flour
- 1 teaspoon granulated sugar
- 1/2 teaspoon salt
- 8 tablespoons/113g butter; frozen
- 6 tablespoons ice water
- 2 teaspoons apple cider vinegar
- 113g/4oz goat cheese; room temperature
- 1 egg; lightly beaten
- 1 large garlic clove; finely grated or minced
- 1 1/2 tablespoons basil; chopped
- Zest of 1 lemon (about 1/2 tablespoon)
- 1/2 teaspoon salt
- Pinch of nutmeg
- 3/4 cup ricotta (about 4 large spoonfulls)



FOR THE DOUGH:

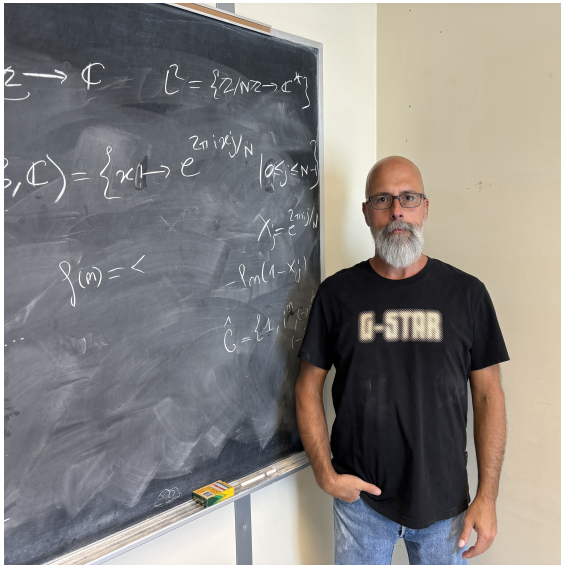
1. In a small bowl, combine 6 tablespoons of ice water and 2 teaspoon of apple cider vinegar. Set aside.
2. In a large mixing bowl, combine flour, sugar, and salt. Cut the butter into small cubes.
3. Toss butter in the flour mixture until all pieces are coated. Using your hands, press the butter into small sheets ensuring that each piece is coated in flour. Refrigerate the bowl for a few minutes if the butter starts to get too soft.
4. Add 4 tablespoon from the water and apple cider vinegar mixture and continue to press the butter into about dime sized sheets until the dough comes together in a shaggy lump. Add more water a couple teaspoons at a time if needed. The dough will be dry, but you should be able to squeeze together a handful of dough without it falling apart.
5. Form the dough into a disk and wrap in plastic wrap. Refrigerate the dough ball for several hours, or ideally overnight.

FOR THE TART:

1. Preheat the oven to 375F. Lightly grease a 9in pie dish.
2. In a small mixing bowl, stir together the goat cheese and egg until smooth and all chunks are gone. Stir in garlic, basil, lemon zest, salt, and nutmeg.
3. Stir in the ricotta.
4. Remove the dough from the fridge and, on a lightly floured work surface, roll out the dough into a 10in round, about 1/4in thick. Fold in half, and half again to transfer your rolled dough to prepared baking dish.
5. Spoon the ricotta filling into the dough making sure to evenly spread to all sides.
6. Arrange asparagus neatly on top.
7. Bake for 25min until crust is golden and sides are set. The center will still be slightly jiggly but it will continue to set as it cools. Enjoy!

INTERVIEW WITH SIDNEY TRUDEAU

Elizabeth van Oorschot



$\delta\epsilon$: What is your name, and how long have you been at McGill?

My name is Sid, and I've been here forever. I started as a student, in 1991, and I've been here ever since. Every day, never left.

$\delta\epsilon$: Tell me about about your background, both personal and academic.

I came here as a student in undergrad, and did the honours undergraduate. In my last year, I did analysis five and six¹ with Professor Klemes. I really enjoyed his classes and did very well in them. He kept me on as a masters student; I did very well there as well, and then I moved on to a PhD under his supervision.

$\delta\epsilon$: What are your favourite things about McGill and Montreal?

I love McGill very much. The students are very smart, and the campus is beautiful. Montreal is a great city, except in January and February... but eight months out of the year, Montreal is great.

$\delta\epsilon$: Are there any courses you particularly enjoy teaching, and if so, why?

I've taught a multitude of courses, all of which I enjoy very much. I've taught analysis, which is very nice, but demanding. Right now I'm teaching calculus 2. I love to teach it, especially since I've been working on some new results that fit well in the calculus 2 curriculum, so near the end of the semester I can share them with the

¹These courses are now retired

students. It's brand new stuff, that essentially nobody else knows, so that's very nice. The results are things the students can grasp and understand; it's stuff that's not beyond them. I would like to think that this motivates people, to understand that there are still some new results out there that are accessible, even if you haven't done a complete graduate degree in mathematics.

$\delta\epsilon$: What is your favourite part of math?

Right now, I have to say series. It's the beginning of a lot of open problems, problems that don't have known solutions. You can essentially write down any series, and you don't know what it converges to. I've been working a lot with series, trying to figure out these things, like what series converge to, can I get series that converge to something, what's going on there. I'm very interested in that.

$\delta\epsilon$: What would you say to a freshman student, who is considering studying math?

Math is very rewarding, I would like to say. The more you do, the more connections you make. If you're serious, you want to do the honours program here. As I said, I came through the honours program. It is more demanding than the majors, but certainly a lot more rewarding, and you want to do as much as you can. You might not think that you're going to do graduate studies, but who knows? I mean, I wasn't going to, and yet, here I am.

$\delta\epsilon$: Do you have any advice for navigating the world of research and academia?

I've had a lot of students ask me about summer research, and my answer is essentially the same as with graduate studies: I took a course with a professor I enjoyed very much, I did well, we had a certain rapport there, and that led to graduate studies under his supervision. I think I would give the same advice to somebody looking to do summer research, or what have you. I mean, if you're in UO, it's probably too early, but when you do higher level courses, you're going to interact with professors who do significant research, and a good relationship there goes a long way.

$\delta\epsilon$: In the past, you have given advice about Loto Quebec on Reddit several times. Could you summarize this advice, for those who have not seen it before?

So, first of all, in those posts I make it clear that I'm not

suggesting that you start gambling, and this is not gambling. This is guaranteed money. I mean, the money isn't that much, especially to an international student who's paying \$60 000 in tuition. I'm up a thousand bucks, though, so it's not insignificant, and you can always donate to charities.

The point is, still ongoing—today [January 28, 2025] is the last day—but they're giving you free money. Essentially you spin a wheel, and they'll give you free money.

In other posts, I had observed that sometimes they offer promotions where they will match the bet you make on sports events, up to \$100. What you want to do is bet \$100 on one team, coupled with a friend who is going to bet on the opposite team. You're guaranteed to essentially make your money back, and each of you

are getting a free \$100 bet on top of that. You're going to again bet that \$100 in the same way, so that one of you is going to win, essentially, that extra \$100 back as well. Amongst the two of you, you made \$100. Again, we're not betting, it's a guaranteed win: a guaranteed \$100. Coupled with the free spins that you are getting, it adds up pretty quickly.

$\delta\varepsilon$: If these promotions constitute a guaranteed way to make money, why do you think Loto Quebec keeps doing them?

They want to bring in new people. They are, of course, hoping that you're going to play that free money, you're going to lose, then you're going to put some more money in and keep losing. The idea is to be smarter than that, and not gamble. Just wait for those promotions. It's money in the bank.

BRAIN TEASER 3

Putnam 1997 A5

Let N_n denote the number of ordered n -tuples of positive integers (a_1, a_2, \dots, a_n) such that $\frac{1}{a_1} + \frac{1}{a_2} + \dots + \frac{1}{a_n} = 1$. Determine whether N_{10} is even or odd.

Solution on page 49

FOURIER ANALYSIS: THE CATALYST OF MODERN ANALYSIS

Nisrine Sqalli and Samy Lahlou

We present in this paper the history of the fundamental concepts, theorems and definitions used in modern analysis which were motivated by the study of Fourier analysis. This will be done chronologically with an emphasis on some mathematicians and papers that had a great impact on the subject.

1 INTRODUCTION

Fourier analysis is one of the most used branches of mathematics in terms of technological advances. It is the result of 200 years of research and collaboration. However, the relevance of Fourier analysis not only lies within its applications, but also in what it inspired throughout time.

In this paper, we will explore the mathematical developments of the 19th and 20th centuries that emerged from the growing interest in Fourier analysis.

We will begin by discussing the origin of Fourier analysis and the role of Joseph Fourier, after whom it is named. Then, we will examine the contributions of Dirichlet, Riemann, and Cantor to Fourier analysis and other branches of mathematics.

2 EARLY STAGES OF FOURIER ANALYSIS

2.1 The Wave Equation

Our story begins in 1747 when Jean Le Rond D'Alembert (1717 – 1783), a French mathematician, derived the *wave equation* [1].

$$\frac{\partial^2 u}{\partial t^2} = c^2 \frac{\partial^2 u}{\partial x^2} \quad (1)$$

The wave equation is a differential equation which governs the vibration of a string with two fixed endpoints. In other words, if you have a function $u(x, t)$ that solves the wave equation (1) such that $u(x, 0)$ corresponds to the initial position of a string, then you can predict the behaviour of the string at any time.

D'Alembert claimed that he had found the solution to the wave equation (1). He expresses it as a sum of two travelling waves going in opposite directions [2]:

$$u(x, t) = \frac{1}{2} [f(x+t) + f(x-t)] + \frac{1}{2} \int_{x-t}^{x+t} g(y) dy \quad (2)$$

where $f(x)$ and $g(x)$ are arbitrary functions. Since $f(x)$ and $g(x)$ are arbitrary, D'Alembert considered that he could represent any initial position of the string, and therefore, has found the *general* solution to the wave equation.

Not long after D'Alembert published his solution, the notorious Swiss mathematician Leonhard Euler (1707 – 1783) objected to D'Alembert's claim to have found the general solution [3]. To understand his objection, we first need to know what D'Alembert and Euler meant by *functions*.

2.2 What is a function ?

At that time, a function is understood to be a *formula* or an *analytic expression* where one can use addition, multiplication, composition with some special functions like $\cos(x)$, $\sin(x)$, e^x ... [4]. For example

$$y = x^2 \cos(x) + 3e^{-x^3}$$

fits the criteria to be called a function. With this definition of functions, it was believed, and admitted, that every function could be represented by a graph but not every graph has an associated function.

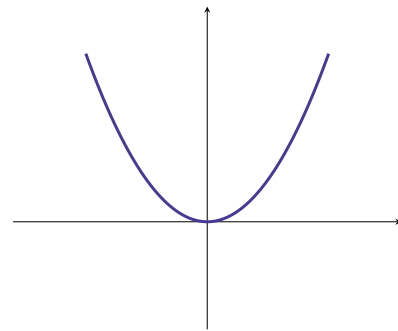


Figure 1:
Graph of the function x^2

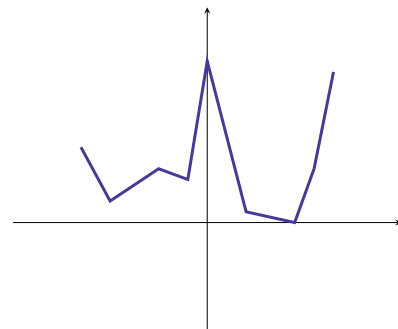


Figure 2:
Graph not associated to a function

Knowing this, we are now able to understand Euler's objection. Any graph models a possible initial position of a string (as long as the end points are fixed on the horizontal axis). But if we consider D'Alembert's solution (2), the initial position of the string (when $t = 0$) is given by $u(x, 0) = f(x)$. Therefore, D'Alembert's claim that you can model any initial position of the string using a function $f(x)$ cannot be true since, as we said earlier, not every graph represents a function. This is Euler's objection.

2.3 Bernoulli's Solution to the Wave Equation

A few years later, in 1755, the Swiss mathematician Daniel Bernoulli (1700 – 1782) also claimed to have solved the wave equation (1), but this time using a different technique. His solution is in the form of an infinite sum of *standing waves* (see Figure 3) [2].

$$u(x, t) = \sum_{m=1}^{\infty} (A_m \cos(mt) + B_m \sin(mt)) \sin(mx) \quad (3)$$

where A_m and B_m are coefficients that are determined by the initial conditions of the problem (that is, the initial position of the string).

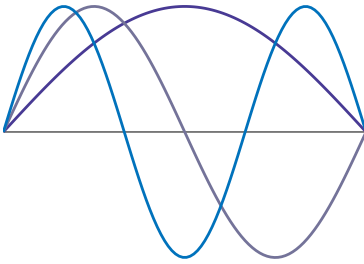


Figure 3: Overlapping standing waves

Similarly to D'Alembert, Euler objected. To understand why, let's consider the initial position of the string according to Bernoulli's solution by plugging $t = 0$ in equation (3):

$$u(x, 0) = \sum_{m=1}^{\infty} A_m \sin(mx)$$

According to Bernoulli, such sum could represent any graph. To prove that Bernoulli was wrong, Euler gave the following argument: Suppose that the initial position of the wave is given by the graph of a function $h(x)$ (expressed using a formula) on the interval $[0, 2\pi]$. Take, for example, $h(x) = x(2\pi - x)$. Bernoulli's claim implies that there exist coefficients A_m such that

$$x(2\pi - x) = \sum_{m=1}^{\infty} A_m \sin(mx)$$

on $[0, 2\pi]$. But according to Euler, if two functions are equal on an interval, they must be equal on the whole real line. In other words, there is only one way to extend a graph associated with a function.

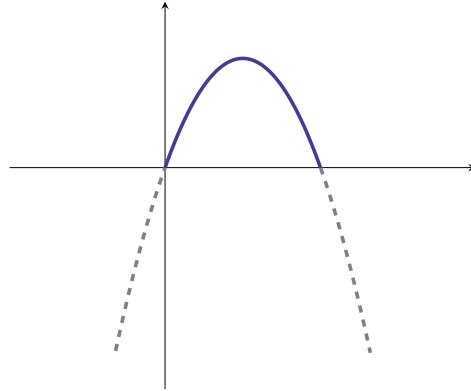


Figure 4:
Graph of the usual function
 $x(2\pi - x)$

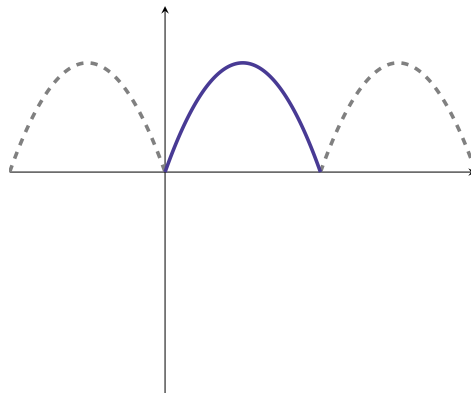


Figure 5:
Graph of the function $x(2\pi - x)$ as
a 2π -periodic function

But since the sine function is 2π -periodic, so is $\sum_{m=1}^{\infty} A_m \sin(mx)$. Therefore, if you were to extend this infinite sum on the real line you will have a 2π periodic graph. On the other hand, if you were to extend $h(x) = x(2\pi - x)$ on the real line, you will simply have a parabola. Since, according to Euler, such extension is unique, we have a contradiction. Therefore, Bernoulli's infinite sum couldn't represent any function $h(x)$. We conclude that equation (3) couldn't be the general solution. Little did they know, Bernoulli was closer to the truth than Euler.

2.4 The Birth of Fourier Analysis

The question of the general solution of the wave equation stayed unanswered for nearly 50 years. In 1822, the French mathematician Jean-Baptiste Joseph Fourier (1768 – 1830) published his famous book *Théorie Analytique de la Chaleur* [5]. In this paper, Fourier studies heat propagation by deriving the *heat equation*

$$\frac{\partial f}{\partial t} = k \frac{\partial^2 f}{\partial x^2} \tag{4}$$

Fourier provides a general solution to this differential equation. To solve his problem with given initial conditions, he must find the coefficients a_n and b_n of the following expression

$$f(x) = \sum_{n=0}^{\infty} a_n \cos(nx) + b_n \sin(nx) \tag{5}$$

where $f(x)$ models the initial heat distribution. In a very non-rigorous 31 page long derivation, Fourier finally finds the following formulas for a_n and b_n , in terms of $f(x)$:

$$a_0 = \frac{1}{2\pi} \int_{-\pi}^{\pi} f(x) dx \tag{6}$$

$$\begin{aligned} a_n &= \frac{1}{\pi} \int_{-\pi}^{\pi} f(x) \cos(nx) dx, \\ b_n &= \frac{1}{\pi} \int_{-\pi}^{\pi} f(x) \sin(nx) dx \end{aligned} \tag{7}$$

But unfortunately, Fourier was not aware that Euler derived nearly identical formula in 1777. After stating these results, Fourier states what we'll call Fourier's Theorem:

“This theorem and the previous one are suitable for all possible functions, whether we can express their nature by known means of analysis, or whether they correspond to curves drawn arbitrarily.” – page 241

In other words, Fourier states that any function or graph can be expressed as a trigonometric series as in equation (5). Given a function $f(x)$, we call the right hand side of equation (5) its *Fourier Series* and the coefficients a_n and b_n the *Fourier coefficients*. This very bold statement, and many other ones, were not proven in any way by Fourier. However, Fourier's book had a huge impact on the mathematical community of his time which led many other mathematicians to attempt to prove Fourier's Theorem.

3 DIRICHLET'S 1829 PAPER

The first proofs attempts of Fourier's Theorem were proposed by the French mathematicians Siméon Denis Poisson (1781 – 1840) in 1820 [6] and Augustin Louis Cauchy (1789 – 1857) with two proofs published in

1827 [7], [8]. However, because of their lack of rigour and numerous errors, their proofs were not accepted.

The first valid and accepted proof was published by the German mathematician Peter Lejeune Dirichlet (1805 – 1859) in 1829 [9]. In his paper, Dirichlet started by pointing out that Cauchy's second proof was wrong. Cauchy used the fact that given two sequences (a_n) and (b_n) , if the limit of their quotient is 1, then $\sum a_n$ converges if and only if $\sum b_n$ converges. To show why it was false, Dirichlet gave the following counterexample:

$$a_n = \frac{(-1)^n}{\sqrt{n}} \left(1 + \frac{(-1)^n}{\sqrt{n}} \right) \quad \text{and} \quad b_n = \frac{(-1)^n}{\sqrt{n}}$$

After this counterexample, Dirichlet started the set up for his proof of Fourier's Theorem. He began by defining a class of functions on which his proof will apply. These functions must satisfy the three following conditions:

1. The function must be integrable.
2. The function must have finitely many maxima and minima.
3. If the function has a jump discontinuity at a point, then its value at this point must be the average of its left and right limits.

Dirichlet, with these clear conditions, gave a proof of Fourier's Theorem that surpassed all of the previous attempts by its rigour. In his proof, Dirichlet made use of the following trigonometric identity:

$$\frac{1}{2} + \cos(x) + \cos(2x) + \dots + \cos(nx) = \frac{\sin\left(\left(n + \frac{1}{2}\right)x\right)}{2 \sin\left(\frac{x}{2}\right)}$$

in which the right hand side is now called the *Dirichlet Kernel*.

After his proof, Dirichlet discussed his three conditions and pointed out that his first condition 1 is nontrivial by giving an example of a function that is not subject to integration. To do so, he defined the function $\varphi(x)$ which is equal to a constant c when x is rational, and to a distinct constant d when x is irrational.

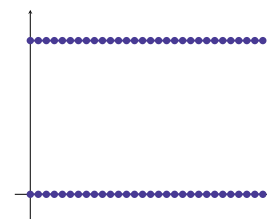


Figure 6: Graph of the Dirichlet Function

For Dirichlet, this function is not subjected to integration since the area under its curve doesn't make any sense. When $c = 1$ and $d = 0$, we call it *Dirichlet's Function*. Notice that with this function, Dirichlet showed that the concept of function in the sense of D'Alembert, Euler and Bernoulli needed to be generalized. As he wrote in a paper in 1837 [10]:

"It is not necessary that y be subject to the same rule as regards x throughout the interval, indeed one need not even be able to express the relation through mathematical operations" – Dirichlet, 1837

Dirichlet set the tone for how mathematical analysis should be done (even though he is more remembered for his work in number theory). His taste for rigour also led him to prove rigorously Abel's Limit Theorem. His proof of Fourier's Theorem was widely accepted in the community [11] and his influence on mathematics is nearly unmatched.

4 RIEMANN'S INTEGRAL AND FUNCTIONS

4.1 Fourier's Theorem Proved?

Dirichlet's proof of Fourier's Theorem was widely accepted in the mathematical community. Even if its proof only focuses on a specific class of functions (the functions satisfying conditions 1, 2 and 3), it turns out that any function that occurs in nature is in this class. Hence, physicists were able to use Fourier's Theorem without worrying about convergence.

In 1854, the German mathematician Georg Friedrich Bernhard Riemann (1826 – 1866) wrote his paper *On the possibility of representing a function by a trigonometric series* (published posthumously in 1867) [11]. In this paper, Riemann argued that Dirichlet's proof was sufficient for the practical case, but the problem of proving Fourier's Theorem in the general case was the still worth studying. To justify that, he gave the two following reasons. First, in addition to physics, the use of Fourier series became more popular in pure mathematics such as number theory. Hence, it would be a mistake to limit ourselves to physics applications only. Secondly, like Dirichlet pointed out in his 1829 paper, trying to prove Fourier's Theorem rigorously leads to profound questions about the foundations of infinitesimal calculus.

4.2 The Riemann Integral

Riemann began his 4th chapter by mentioning that integral theory is still very uncertain. He then asks a clever question:

Also zuerst: Was hat man unter $\int_a^b f(x) dx$ zu verstehen?

Picture from *On the possibility of representing a function by a trigonometric series* by Riemann [11]

which translates to *"But first, what does $\int_a^b f(x)dx$ mean?"* Until that point in time, mathematicians have been talking about integrals recurrently, however the integral had no robust definition. Before Riemann's 1867 paper, the closest definition we had was given by Cauchy in his 1823 book [12]. However, his integral wasn't widely accepted since it only applies to continuous functions or functions with finitely many discontinuities. This left the door open for other mathematicians to broaden the definition of the integral and better accommodate it to Dirichlet's definition of a function and handle infinitely many discontinuities.

The Riemann integral can indeed handle infinitely many discontinuities. To illustrate the power of his new integral, Riemann gave a function with infinitely many discontinuities that is still integrable, which we call *Riemann's Pathological Function*. He defined it as follows:

$$f(x) = \frac{(x)}{1} + \frac{(2x)}{4} + \frac{(3x)}{9} + \dots = \sum_1^{\infty} \frac{(nx)}{n^2}$$

where $x \mapsto (x)$ denotes the periodic function equal to the identity function on $[-\frac{1}{2}, \frac{1}{2})$ with period 1. This function is integrable and has infinitely many maxima and minima. Does this ring a bell?

If you remember Dirichlet's conditions, here we have a function that satisfies condition 1 but does not satisfy condition 2. This proves that condition 1 cannot imply condition 2. However, Riemann proved rigorously that the converse is true. Namely, if a function has finitely many maxima and minima, then it is integrable. This shows that condition 1 doesn't need to be cited in Dirichlet's conditions. Simply conditions 2 and 3 suffice.

4.3 A New Shift in Analysis

The end of Riemann's paper was filled with examples of functions that test the limits of Dirichlet's conditions in different ways. We have already seen a prime example of such functions with Riemann's Pathological Function (Figure 8). He presented functions with infinitely many maxima and minima, and in addition, gave a function similar to his pathological function (Figure 8). It is a non-integrable function which still has a Fourier series that converges and diverges on a dense subset of \mathbb{R} . He found its Fourier series by crafting a trigonometric series directly from the expression

of the function instead of integrating the function to find the Fourier coefficients.

In the 19th century, mathematical analysis took a radical turn. A new trend started emerging: imagining weird-behaving functions to push the limits of theorems and definitions. Riemann's paper was a paramount example of this. Notice that Dirichlet's function is perfectly aligned with this trend. Other famous examples can be cited from this period: Thomae's Function (1872), which is continuous only on the irrationals, and Weierstrass's Function (1875), which is continuous but nowhere differentiable². This naturally lead to the study of sets of discontinuities of weird behaving function and ultimately to sets in general.

5 CANTOR'S STUDY OF SETS

5.1 The Uniqueness Theorem

The mathematician who pushed the concept of sets to another level is Georg Cantor (1845 – 1918) in the late 19th century. As he was working at the University of Halle, Cantor heard about the uniqueness problem for trigonometric series in 1869 by his colleague, Eduard Heine, who was working on it. Their goal was to show that if a function has a representation as a trigonometric series, then such a representation is unique (i.e., it cannot be represented by two trigonometric series with different coefficients).

After only one year, in 1870, Cantor published a proof to the Uniqueness Theorem for trigonometric series, where he assumed the convergence of the series for all values of x taken between 0 and 2π [14]. The following year, in 1871, Cantor improved his theorem and showed that it still holds even if you don't necessarily assume the convergence of the series for finitely many points [15].

Nevertheless, Cantor was convinced that this was too restrictive. He believed that the Uniqueness Theorem holds even if the convergence is not assumed of infinitely many points. However, those "infinitely many points" cannot be arbitrarily distributed. For example, if you don't assume the convergence on the infinitely many points that constitute the interval $[0, 2\pi]$, then the theorem obviously doesn't hold anymore. Thus, Cantor needed to describe precisely the *systems of points* (he would use the term *set* only a decade later) that may be infinite and on which the convergence of the series can be ignored.

This is exactly what Cantor did the following year, in

²For more details about these functions, we refer you to Chapters 4 and 5 of Understanding Analysis by Stephen Abbott [13].

1872 [16]. Cantor knew that he had to be rigorous enough to be able to make such an improvement to his theorem. Hence, he started from the very beginning by defining the real numbers as equivalence classes of rational Cauchy sequences. After that, Cantor defined the following notions. A *neighborhood* of a point is any interval that contains the point. A *limit point* of a system P is a point such that any of his neighborhoods contain infinitely many points of the system P . Lastly, an *isolated point* of a system P is any point of the system that isn't a limit point of P . These definitions are very similar to the ones we use today in topology. To make everything clearer, take, for example, the system P containing the reciprocals of the integers. We can visualize this system in Figure 11.



Figure 11: Illustration of the system containing the points $1, \frac{1}{2}, \frac{1}{3}, \frac{1}{4}, \dots$

The point 0 is a limit point of P (even if it is not contained in P) and any element of P is an isolated point.

From these notions, he defined the derived system of P , called P' , to be the system of the limit points of P . In our previous example, P' would be the system containing the point 0. Applying this operation n times to a system P gives what he calls the n th derived system $P^{(n)}$ from P . After all these definitions, Cantor was finally able to state and prove his theorem. Here is how he stated it in his paper:

Theorem 1 (Cantor). *Given two Fourier series that converge on $[0, 2\pi]$ except on a system P where $P^{(n)}$ is finite for a whole number n , if both series are equal then their respective Fourier coefficients are equal.*

5.2 A General Theory of Sets

However, a disturbing question arose: Why would this theorem hold for some infinite systems and not others?

This led to Cantor to question himself on the nature of infinity. In 1874, Cantor proved, using what we now call the Nested Interval Property, that there is no one-to-one correspondence between the natural numbers and the real numbers. He was indeed beginning to explore the idea of different *kinds* of infinity. Three years later, in the same spirit, Cantor showed this time that there exist a one-to-one correspondence between the real numbers and any n -dimensional space.

Combining all of these results about what he now calls *sets*, and after creating more tools to explore his new ideas (such as transfinite numbers and their transfinite arithmetic), Cantor published all of these results in a 1883 paper called *Foundations of a General Theory of Sets* [17].

6 WHAT ABOUT NOW?

As it was said at the end of our discussion on Riemann, the study of sets in analysis became more and more common at the end of the century. Even if we decided to focus on Cantor, other mathematicians started to define some way of describing sets. One such mathematician is Giuseppe Peano (1858 – 1932) who defined to notion of inner and outer content of a set. His work was then continued by the French mathematicians Camille Jordan (1838 – 1922) and especially Emile Borel (1871 – 1956) who created the notion of *measure* [18].

From this new theory of measures, Lebesgue extended Borel's work by creating a whole new theory of functions and integration. Lebesgue's integral is still used today as the standard integral in Analysis because of its generality and also because of all the nice convergence theorems that Riemann's integral lacks of. It also turns out that today's most advanced results on the original goal of proving Fourier's Theorem and improving Dirichlet's conditions are stated in the language of Lebesgue's analysis. Two such results are the Riesz-Fischer Theorem, proved in 1907, and Carleson's Theorem, proved in 1966.

Theorem 2 (Riesz-Fischer Theorem). *A function is in L^2 if and only if its Fourier series converges in the sense of L^2 .*

Theorem 3 (Carleson's Theorem). *Any function in L^2 has Fourier series that converges almost everywhere.*

We find that the main takeaway of this paper is how a simple idea coming from a single person can impact a whole research field. Fourier analysis is now a key component in mathematics, physics, quantum computation and even music softwares. However, it would be mistaken to think that this is a one in a million phenomenon. This happened and will happen a numerous amount of times in mathematics. One can think of Euclid's famous fifth postulate, which preoccupied the minds of mathematicians for centuries and led to the study of non-euclidean geometry. Another example would be Fermat's Last Theorem which led to the development of algebraic number theory. This is where our story ends.

7 FURTHER READINGS

If you are interested in learning more about this topic, the full version of this paper with additional sections and discussions can be found on the following website: <https://samylahlou.com/paper.html>. For more informations about a specific section, here are the books and sources we relied on the most for the different parts. Section 2 is mostly based on the first half of the section *Fourier Analysis* of the book the *Mathematical Experience* [3]. More details about D'Alembert's and Bernoulli's solutions can be found in the first chapter of the book *Fourier Analysis: An Introduction* [2]. The beginning of Section 3 is based on Sections 3.5 and 3.9 of the book *From Calculus to Set Theory* (which contains a few errors that we corrected) [19]. The rest of the section is based on Dirichlet's 1829 paper [9] and the beginning of Riemann's 1867 paper [11]. Section 4 is solely based on Riemann's 1867 paper which is very readable and self-contained. For Section 5, we relied on sections 5.1, 5.2 and 5.3 of the book *From Calculus to Set Theory* [19] and Cantor's 1872 paper [16].

REFERENCES

- [1] D'Alembert, J. *Recherches sur la courbe que forme une corde tendue mise en vibration.* (1747)
- [2] Stein, E. & Shakarchi, R. *Fourier Analysis: An Introduction.* (Princeton University Press, 2011), <https://books.google.ca/books?id=FA0c24bTfGkC>
- [3] Davis, P. & Hersh, R. *The Mathematical Experience.* (Houghton Mifflin, 1998), <https://books.google.ca/books?id=1MdZ84dWNnAC>
- [4] Dunham, W. *The Calculus Gallery: Masterpieces from Newton to Lebesgue.* (Princeton University Press, 2005), <https://books.google.ca/books?id=QnXSqvTiEjYC>
- [5] Fourier, J. *Théorie analytique de la chaleur.* (Didot, 1822), <https://books.google.ca/books?id=TDQJAAAAIAAJ>
- [6] Poisson, S. *Suite du mémoire sur les intégrales définies....* (1820)
- [7] Cauchy, A. *Mémoire sur les développements des fonctions en séries périodiques.* (1827)
- [8] Cauchy, A. *Sur les résidus des fonctions exprimées par des intégrales définies. Oeuvres (2).* 7 pp. 393 (1827)
- [9] Dirichlet, P. *Sur la convergence des séries trigonométriques qui servent à représenter une fonction arbitraire entre des limites données.*

- Journal für die reine und angewandte Mathematik* pp. 157-169 (1829). <https://doi.org/10.48550/arXiv.0806.1294>
- [10] Dirichlet, P. Ueber die Darstellung ganz willkürlicher Funktionen durch Sinus-und Cosinusreihen. *Repertorium Der Physik, Bd. I, S.* pp. 252-174 (1889)
- [11] Riemann, G. *Über die Darstellbarkeit einer Funktion durch eine trigonometrische Reihe (Habilitationsschrift). Gö. Tt. Abh.* 13 pp. 272-287 (1867)
- [12] Cauchy, A. *Résumé des leçons données à l'école royale polytechnique sur le calcul infinitésimal.* (Imprimerie royale, 1823)
- [13] Abbott, S. *Understanding Analysis.* (Springer,2010), <https://books.google.ca/books?id=jfMD1NqvWfsC>
- [14] Cantor, G. *Beweis, dass eine für jeden reellen Werth von x durch eine trigonometrische Reihe gegebene Function $f(x)$ sich nur auf eine einzige Weise in dieser Form darstellen lässt.* *Journal Für Die Reine Und Angewandte Mathematik.* 1870, 139-142 (1870), <https://doi.org/10.1515/crll.1870.72.139>
- [15] Cantor, G. *Notiz zu dem Aufsätze: Beweis, dass eine für jeden reellen Werth von x durch eine trigonometrische Reihe gegebene Function $f(x)$ sich nur auf eine einzige Weise in dieser Form darstellen lässt.* *Bd. 72, Seite 139 dieses Journals.* *Journal Für Die Reine Und Angewandte Mathematik.* 1871, 294-296 (1871), <https://doi.org/10.1515/crll.1871.73.294>
- [16] Cantor, G. *Über die Ausdehnung eines Satzes aus der Theorie der trigonometrischen Reihen.* *Mathematische Annalen.* **5**, 123-132 (1872)
- [17] Cantor, G. *Fondements d'une théorie générale des ensembles.* (1883)
- [18] Kupka, J. *Measure theory: the heart of the matter.* *The Mathematical Intelligencer.* **8**, 47-56 (1986)
- [19] Grattan-Guinness, I. & Bos, H. *From the Calculus to Set Theory, 1630-1910: An Introductory History.* (Princeton University Press,2000), <https://books.google.ca/books?id=OLNeNIbD3jUC>

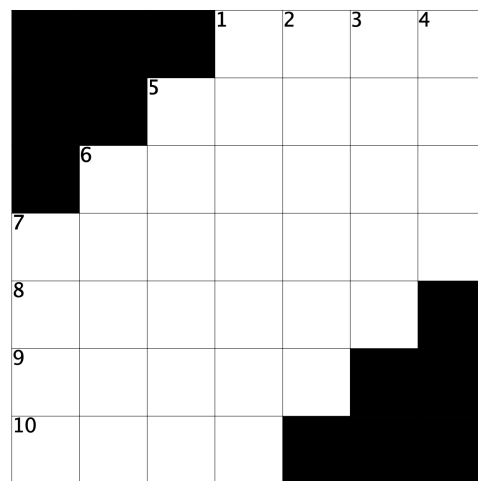
JOKES

We hope these jokes aren't too *complex* to understand:

- Yesterday, I went to a restaurant with my complex number friend, needless to say $\frac{i}{8} \dots$
- Complex numbers are complicated! Or maybe I'm just imagining things...
- Complex numbers are all fun and games until someone loses an $i \dots$

CROSSWORD

Helena Heinonen



ACROSS

1. Negative value?
5. μ
6. What you want your roommate to do, say
7. Comes from, as a corollary
8. They might be used for ball packing, informally
9. Reacts to a bad grade, maybe
10. Dot on the eye?

DOWN

1. Abhor, on social media
2. Apes
3. Makes a pot of French press
4. Typical Bernoulli trial
5. Moderately
6. Coffee mug, topologically
7. No muss, no ____

SOLUTION TO PUZZLES

BRAIN TEASER 1

All brain teasers courtesy of Hussin Suleiman

Since the table is circular, it is natural to think of copycat strategies for both players. Indeed, if Alice places a coin on one end of the table, Bob can place his coin on the opposite end of the table, “copying” Alice’s moves. Then, Bob would always have a legal move after Alice plays. But what if Alice places her first coin in the centre of the table? Now, Bob cannot “copy” Alice’s move, as he is not allowed to put a coin in the centre on top of Alice’s coin. So, he must put his coin somewhere else on the table. But then, Alice can make use of a copycat strategy to win the game. No matter where Bob puts his coins, Alice can always put her coins on the opposite end of the table, until Bob eventually runs out of space to place new coins. Therefore, Alice has the winning strategy.

BRAIN TEASER 2

Computing the determinant of a 4 by 4 matrix can already be quite tedious, so what are we to do with a 2008 by 2008 matrix? Clearly, a brute force approach will not work. Instead, recall that we only care about whether or not the determinant is 0. Thus, we consider simple conditions that ensure the determinant of a matrix is 0. Clearly, if all entries of a given row are 0, then the determinant is 0. Moreover, adding or subtracting a multiple of one row to another does not change the determinant. Thus, if two rows of the matrix are identical, then subtracting one row from the other yields a row with all 0 entries, giving a determinant of 0. So, Barbara only needs to force two rows to be identical in order to win. This motivates Barbara’s strategy.

Consider rows 1 and 2 of the matrix. Whenever Alan places a number in a column c of row 1 or 2, Barbara places the same number in the column c of the opposite row. If Alan places a number anywhere else in the array, Barbara plays whatever she wants, without changing rows 1 or 2. Note that because there are $2006 \cdot 2008$ entries outside of the rows 1 and 2, which is an even number, Barbara will always have an entry in which to play when Alan chooses not to play in rows 1 or 2. Eventually, Alan will have to play in rows 1 and 2, at which point Barbara applies her pairing strategy to win. So, Barbara has the winning strategy.

BRAIN TEASER 3

Denote the equation $\frac{1}{a_1} + \frac{1}{a_2} + \dots + \frac{1}{a_n} = 1$ by (*).

Since we only care about the parity of N_{10} , we can consider grouping the solution tuples by pairs until either all solutions are paired, or one solution is left over.

Observe that (*) does not depend on the order of the terms in the sum. Thus, if $a_1 \neq a_2$ and $(a_1, a_2, a_3, \dots, a_{10})$ is a solution tuple for (*), then so is $(a_2, a_1, a_3, \dots, a_{10})$; this gives us a pair of solutions. Similarly, if $a_3 \neq a_4$ then we can interchange a_3 and a_4 to get a new solution, giving another pair of solutions. The same can be said for $a_5 \neq a_6$, $a_7 \neq a_8$, and $a_9 \neq a_{10}$. So, the parity of N_{10} is just the parity of the number of solution to the equation obtained from (*) by setting $a_1 = a_2$, $a_3 = a_4$, $a_5 = a_6$, $a_7 = a_8$, and $a_9 = a_{10}$, namely:

$$\frac{2}{a_1} + \frac{2}{a_3} + \frac{2}{a_5} + \frac{2}{a_7} + \frac{2}{a_9} = 1 \quad (**)$$

It follows from the same kind of pairing argument that the parity of the number of solutions of (**) is the same as that of the number of solutions to the equation obtained from (**) by setting $a_1 = a_3$ and $a_5 = a_7$, namely:

$$\frac{4}{a_3} + \frac{4}{a_5} + \frac{2}{a_9} = 1 \quad (***)$$

Finally, applying the same pairing argument one more time, the parity of the number of solutions of (***) is the same as that of the equation obtained from (***) by setting $a_1 = a_5$:

$$\frac{8}{a_1} + \frac{2}{a_9} = 1 \quad (***)$$

So, to find the parity of N_{10} , it suffices to find the parity of the number of solutions to (***) . We now solve the equation (***) in positive integers:

$$\frac{8}{a_1} + \frac{2}{a_9} = 1 \iff 8a_9 + 2a_1 = a_1 \cdot a_9 \iff a_1 \cdot a_9 - 2a_1 - 8a_9 = 0 \iff (a_1 - 8)(a_9 - 2) = 16$$

Thus, $(a_1 - 8) | 16$. Note that 16 has 5 positive divisors: 1, 2, 4, 8, and 16. So, $a_1 - 8$ has 5 possible positive values, each of which yields a positive value for a_1 and a_9 ; this yields 5 solution tuples. Moreover, $a_1 - 8 > -8$ and if $a_1 - 8$ equals any of $-1, -2, \text{ or } -4$, then the value obtained for a_9 is negative, a contradiction. Thus, equation (***) has 5 solution tuples. In particular, it has an odd number of solution tuples; it follows that N_{10} is also odd.

SUDOKUS

9	7	5	6	1	3	8	2	4
1	3	8	4	7	2	6	9	5
6	4	2	8	9	5	1	3	7
4	5	3	9	2	8	7	6	1
7	2	6	5	4	1	9	8	3
8	1	9	7	3	6	4	5	2
3	8	7	1	5	9	2	4	6
5	6	4	2	8	7	3	1	9
2	9	1	3	6	4	5	7	8

page 15

6	2	8	5	3	4	9	1	7
5	1	9	8	7	2	4	3	6
4	3	7	9	1	6	2	5	8
8	6	5	2	4	7	1	9	3
3	9	2	1	8	5	7	6	4
7	4	1	6	9	3	5	8	2
2	5	4	3	6	9	8	7	1
1	7	6	4	5	8	3	2	9
9	8	3	7	2	1	6	4	5

page 30

CROSSWORD

				1	2	3	4	
				D	E	B	T	
			5	M	I	C	R	O
	6		D	I	S	H	E	S
7	F	O	L	L	O	W	S	
8	U	N	D	I	E	S		
9	S	U	L	K	S			
10	S	T	Y	E				

CREDITS

In alphabetical order

Editors-in-Chief

- Helena Heinonen
- Hy Vu

Editors

- Elizabeth van Oorschot
- Aahaan Rawal
- Aditya Sharma

Cover Art & Design

- Nicholas Hayek
- Claire Zhang

The Graduate Review Board

- Hazem Hassan
- Antoine Labelle
- Pengqi Liu
- Vincent Painchaud

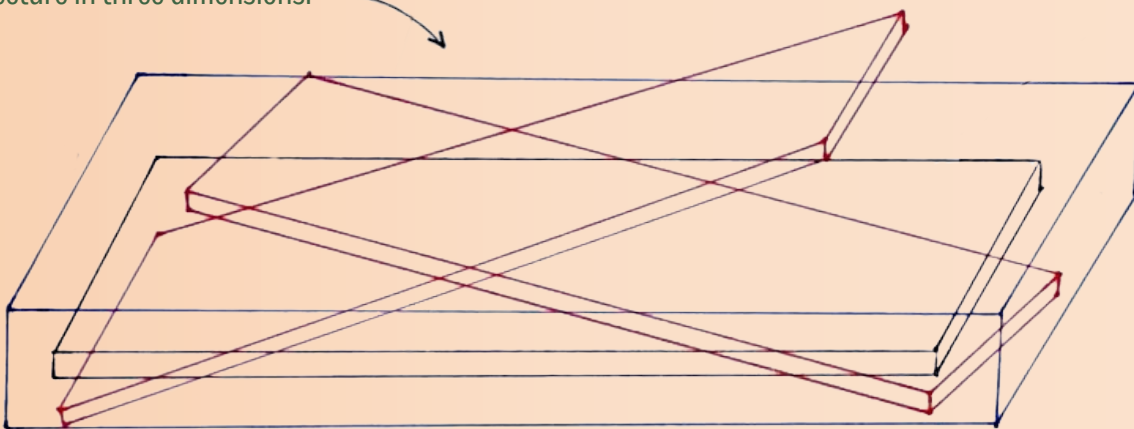
Directors

- Nicholas Hayek
- Charlotte Weiss

ACKNOWLEDGEMENTS

The production of this issue would not have been possible without the gracious help of many contributors. We'd like to thank Léo Belzile, current HEC Professor and editor-in-chief circa 2014 of *The Delta Epsilon*, for recovering old files and Charlotte Weiss and Nicholas Hayek for spending their summer compiling them. We appreciate all the authors for sharing their hard work with the mathematical community and thank the entire graduate review board for volunteering their time to peer-review all articles for mathematical accuracy. Special thanks to Jean-Pierre Mutanguha and Sidney Trudeau for agreeing to share their wise words and advice in interviews with *The Delta Epsilon*. We are grateful to SUMS and AUS for their generous financial support to make the physical printing of this journal possible. And of course, we thank the readers of this journal, without whom this publication would be futile.

FIGURES: The Kakeya Conjecture posits that, in any plane, a set of points that allows a line segment to be rotated through all directions (called a "Kakeya set") must have positive area. This conjecture is closely tied to problems in geometry and analysis. Josh Zahl and Hong Wang have recently claimed a proof of the Kakeya Conjecture in three dimensions.



Wang, H., & Zahl, J. (2025). Volume estimates for unions of convex sets, and the Kakeya set conjecture in three dimensions. arXiv:2502.17655. <https://doi.org/10.48550/arXiv.2502.17655>